Space Missions Minor - Engineering Case study

AE3538 - Venturing into the Heliosphere

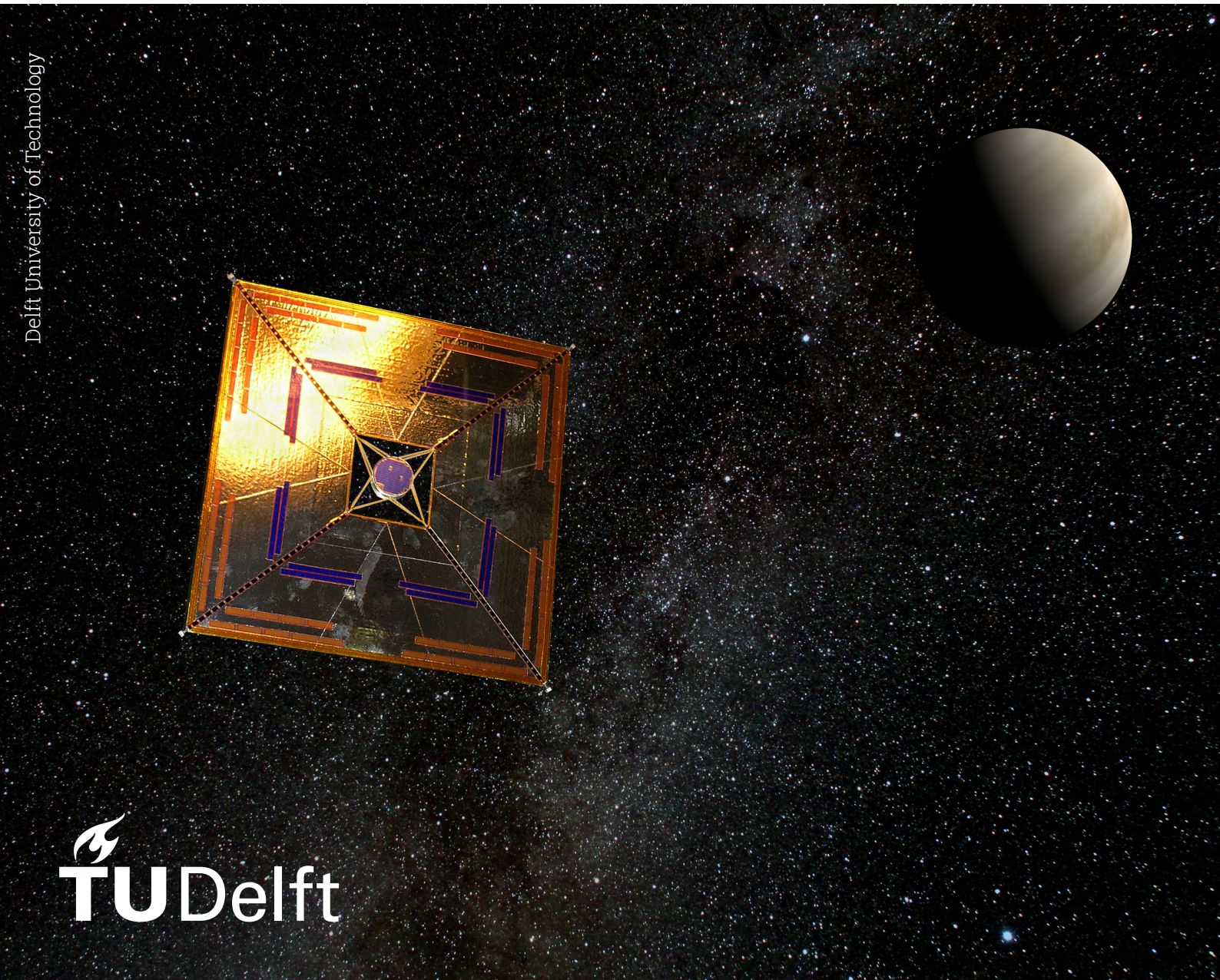

Delft University of Technology

TU Delft

Space Missions Minor - Engineering Case study

AE3538 - Venturing into the Heliosphere

by

Student Name	Student Number
Isabelle Joosten	
Raul Cotar	
Fanni Fiedrich	
Samuel van Erk	
Finn Heijink	
Iorcan Jagt	
Huub Reitsma	
Jelle van der Meer	

Mission Client:	Michel van Pelt
Scientific Tutor:	Marie van de Sande
Engineering Tutor:	Iklim Akay
Project Duration:	November, 2023 - January, 2024
Faculty:	Faculty of Aerospace Engineering, Delft

Cover:	A shiny golden-hued square with a small spacecraft attached in space with a planet in the background by The Conversation [1]
Style:	TU Delft Report Style, with modifications by Daan Zwaneveld

TU Delft

Contents

Nomenclature

Abbreviations

Abbreviation	Definition
ADCS	Attitude Determination & Control Subsystem
ARW	Angular Random Walk
AU	Astronomical Unit equal to 1.495979e+8km
B €	1 billion euro
BOL	Beginning-of-Life
(k)bps	(kilo) bits per second
C&DH	Command and Data Handling
ΔV	Delta V / Velocity change
DSA	One of Estrack's Deep Space Antennas (ground station)
DSS	One of NASA's Deep Space Stations (ground station)
EOL	End-of-Life
ESA	The European Space Agency
Estrack	The European Space Tracking ground station network
FEEP	Field Emission Electric Propulsion
FOG	Fiber Optics Gyroscope
HGA	High Gain Antenna
IMU	Inertial Measurement Unit
JHIP	Johns Hopkins Interstellar Probe
JUICE	Jupiter Icy Moons Explorer
LGA	Low Gain Antenna
LNA	Low-Noise Amplifier
M €	1 million euro
MEMS	Micro Electro-Mechanic System
MLI	multi-layer insulation
Mbps	mega bits per second
NASA	The National Aeronautics and Space Administration
OBC	On-Board Computer
OBDH	On-Board Data Handling
RF	Radio Frequency
RTG	Radioisotope Thermoelectric Generator
SoC	System on a Chip
SpW	SpaceWire
SSR	Solid State Recorder
W	Watt

1

Introduction

Prepared by Huub Reitsma and proof-read by Iorcan Jagt

In the history of humankind only three spacecraft have ever ventured into interstellar space [2]. However, none of them have been equipped for proper exploration of interstellar space, all of these five spacecraft were equipped for exploring the outer planets and objects of the solar system but not for interstellar space and/or the heliosphere. In part due to this lack of in-situ measurements of the interstellar medium and the heliosphere, not a lot is known of these areas.
This report aims to provide a detailed overview of the concept of an interstellar heliosphere probe to investigate the heliosphere and the interstellar medium. This report will examine the requirements that are needed for such a spacecraft and explain why these requirements exist. Moreover, a component level description of the various subsystems typically involved in spacecraft manufacturing will be provided. With these subsystems, estimations of the mass, cost, power and data will be given when appropriate in an overview of all the subsystems.

2 Requirements

Prepared by Iorcan Jagt and proof-read by Fanni Fiedrich

In this chapter the different requirements given by the client will be explained and divided into sub-categories.

2.1. The Requirements

For the design of a spacecraft capable of going to the edge of the heliosphere, multiple requirements were given by the client. These requirements serve as a baseline for the initial design considerations. If all goes well every requirement will be met at the end of the design process. The requirements can be divided into 3 categories: Client requirements, Science requirements and technical requirements. Client requirements are requirements that are requests of the client to improve chances of this mission proposal being accepted by ESA. The science requirements are requirements that influence what kind of science the spacecraft needs to perform. Finally the technical requirements affect the mechanical aspect of the mission. The different requirements can be seen in Table 2.1.

Client Requirements	Science Requirements	Technical Requirements
The spacecraft shall launch no later than 2035.	The payload shall investigate interactions within the heliosphere.	The payload shall weigh less than 25 kg.
The spacecraft shall reach a distance of 200 Astronomical units (AU).	The payload shall perform experiments within the heliosphere.	The technology used shall have a Technology Readiness Level (TRL) of 5 or above.
The spacecraft shall reach the 200 AU within 30 years from launch.	The payload shall determine the composition of the ISM.	
The mission shall cost no more than 1 billion Euros.		
The mission shall use exclusively European technology.		
The spacecraft shall launch with an European launcher (Ariana 62, Ariana 64 or Vega-E).		

Table 2.1: The requirements sorted into three categories: Client requirements, Science requirements and Technical requirements

During the design process it was concluded that two requirements would be killer requirements. These are requirements that are impossible to be met. The two requirements are:

- The spacecraft shall use exclusively European technology.
- The technology used shall have a Technology Readiness Level (TRL) of 5 or above.

Together with the client it was decided that for these requirements do not have to be met if sufficient arguments are given. These arguments are explained in chapter 4 and chapter 9.

3

Orbit Determination

Prepared by Jelle van der Meer and proof-read by Isabelle Joosten
In this chapter different routes through the solar system are analysed to determine an efficient and feasible route that the spacecraft can take to reach 200 AU within stated requirements. Different routes are discussed and important parameters are calculated to make a well rounded decision on the route that could be taken. The analysis is done under certain assumptions to allow simplification of the calculations as well as provide an estimate for the required ΔV and time. This is also to ensure a first approximation that can be used to obtain a concept for the Heliosphere probe.

3.1. Routes from past missions

In order to narrow down the most efficient routes in terms of ΔV, it is convenient to have a look at routes that similar missions have taken. The routes of eight different missions/concepts are provided in Table 3.1, together with the planets that had been used for gravity assists.

Mission	Flight path	Sun	Mercury	Venus	Earth	Mars	Jupiter	Saturn	Uranus	Neptune	Pluto	Gravity Assits	Source
Voyager 1	Earth - Jupiter - Saturn											Jupiter, Saturn	[3]
Voyager 2	Earth - Jupiter - Saturn - Uranus - Neptune											Jupiter, Saturn, Uranus, Neptune	[3]
New Horizons	Earth - Jupiter - Pluto											Jupiter	[4]
Pioneer 10	Earth - Jupiter											Jupiter	[5]
Pioneer 11	Earth - Jupiter - Saturn											Jupiter, Saturn	[6]
Galileo	Earth - Venus - Jupiter											Venus	[7]
Cassini	Earth - Venus - Jupiter - Saturn											Earth, Venus, Jupiter	[8]
ESA IHP	Earth - Sun											Earth	

Table 3.1: Mission flight paths utilising gravity assists

From Table 3.1 it can be seen that missions going far out into the solar system such as the Voyagers and Pioneers, utilised Jupiter and Saturn for their gravity assists. For missions going towards the outer planets, Venus was also an option which can be counter-intuitive as Venus is an inner planet. Jupiter, Saturn and Venus are the planets utilised most often for gravity assists. From this table the first preliminary routes can be determined for further analysis. The analysis in Chapter 3 is done on six different routes, those routes are: ***Route 1:*** Earth - Venus - Jupiter, ***Route 2:*** Earth - Venus - Saturn, ***Route 3:*** Earth - Venus - Jupiter - Saturn, ***Route 4:*** Earth- Jupiter - Saturn, ***Route 5:*** Earth - Saturn, ***Route 6:*** Earth - Jupiter. Those six routes will be analysed on time of travel and the amount of ΔV needed to perform the route. The ΔV provides an indication of the amount of energy and speed that is needed and can be used to approximate the size of the propulsion subsystem.

3.2. Assumptions and Simplifications

To obtain an approximation for the time of travel and the amount of ΔV it is important to state the assumptions and simplifications made to the calculations. The routes are planned out using two major methods - **Method 1:** interplanetary Hohmann transfers, and **Method 2:** gravity assists. The routes therefore consist of Hohmann transfers between planets, based on patched conics, with gravity assists at certain planets along the route. The assumptions and simplifications are:

Assumptions:

- Interplanetary Hohmann transfers only
- un-powered gravity assists
- Close-approach for gravity assists possible
- 2D Keplerian orbits and planes
- existing launch windows

Simplifications:

- ΔV gained from gravity assists is added to the velocity at end-route at final planet
- Average constant velocity is taken from departure at final planet to 200 AU
- Route consists of a maximum of 3 different planets excluding earth

The assumptions and simplifications have the following implications: planets follow circular orbits around the sun; the routes exist in 2D space; a close approaches is defined as 100000 km altitude from Jupiter and Saturn, 50000 km from Neptune and Uranus, and 3000 km from the other planets; the time of travel after the final planet en-route is taken from an average velocity to obtain a crude approximation for travel time to 200 AU; and finally, a limit on the amount of planets per route to prevent unreasonable launch windows within our requirements. Taking the above into account the routes can be analysed by means of a python script which can be found in Appendix A.

3.3. Results

3.3.1. Hohmann transfers (Earth - Planet)

To start the analysis, the results of the Hohmann transfers from Earth to each planet are given. This provides an indication of the preferable options. It is also convenient to do this as two of the assumed routes (route 5 and 6) only involve Earth and one other planet, indicating that one needed Hohmann transfer is sufficient.

Hohmann transfer to:	ΔV Injection [km/s]	Transfer time [days/years]
Mercury	5.55	105 / 0.29
Venus	3.49	146 / 0.40
Mars	3.60	259 / 0.71
Jupiter	6.30	998 / 2.73
Saturn	7.29	2220 / 6.08
Neptune	7.98	5847 / 16.02
Uranus	8.25	11242 / 30.80

Table 3.2: Hohmann transfer from Earth to Planet

From the table one can observe that the ΔV needed to reach Venus and Mars is around 3.5 km/s. Reaching Mercury requires 1.5 times more, and reaching the other planets requires around 2 times more ΔV. The travel time from earth towards the inner planets is less then a year, 2.7 to 6.08 years for Jupiter and Saturn respectively and Neptune and Uranus both more then 10 years. Mercury is not preferred as it requires a relatively high ΔV just to arrive closer to the sun. Jupiter and Saturn require two times more ΔV but allows the spacecraft to travel far outward of the solar system in a reasonable time of three to six years. With the Hohmann transfers alone, the velocity of the spacecraft is still too low to allow the spacecraft to escape the solar system. The analysis will be extended by analysing the gravity assists.

3.3.2. Gravity assist analysis

The amount of ΔV gained from a gravity assists depends on the central body, the distance to the central body, and the relative motion between the spacecraft and the central body. In Appendix A,

graphs plotting the ΔV gained against distance to the planet are shown for each planet (see Figure A.4 and Figure A.5). The graphs show that the closer the spacecraft is to the central body, the larger the gain in ΔV is. For further analysis the maximum value for ΔV gain is used. Comparing the three planets close to earth, Venus is able to provide a ΔV larger then 4.7 km/s while Mars and Mercury only provide around 3 km/s at same distance. Comparing the four remaining planets, Jupiter and Saturn both provide a ΔV of 10 km/s or higher, while Neptune and Uranus provide around 7 and 8 km/s of ΔV respectively, even with an already closer distance.

Comparing the planets, the best candidates for gravity assist will be Venus for planets close to earth, and Jupiter and Saturn for planets far from earth. Furthermore, the analysis shows if one gravity assist of the planet is enough to put the spacecraft on an escape trajectory after the Hohmann transfer, these results are provided in Table 3.3. It can be seen that the three closest planets do not provide sufficient ΔV with one gravity assist while the four remaining planets do, reinforcing the choice for routes 5 and 6.

Planet	GA sufficiency
Mercury	INSUFFICIENT
Venus	INSUFFICIENT
Mars	INSUFFICIENT
Jupiter	SUFFICIENT
Saturn	SUFFICIENT
Neptune	SUFFICIENT
Uranus	SUFFICIENT

Table 3.3: Gravity assist sufficiency for escaping the solar system

3.3.3. Interplanetary Hohmann transfers [Complete Routes]

Building upon subsection 3.3.1 and subsection 3.3.2, the orbits are extended to interplanetary Hohmann transfers, as the analysis for routes 1 to 4 involve multiple planets. The results are presented in Table 3.4.

Route	ΔV injection [km/s]	Transfer time [days/year]	Transfer time to 200 AU [years]
1: (Earth-Venus-Jupiter)	11.58	1078 / 2.95	59.6
2: (Earth-Venus-Saturn)	19.46	2279 / 6.24	70.13
3: (Earth-Venus-Jupiter-Saturn)	28.74	4745 / 13.0	51.57
4: (Earth-Jupiter-Saturn)	22.21	4665 / 12.78	66.25
5: (Earth-Saturn)	7.29	2220 / 6.08	105.6
6: (Earth-Jupiter)	6.30	998 / 2.73	88.7

Table 3.4: Interplanetary Hohmann transfer ΔV and transfer time

Comparing the different routes by their ΔV and their transfer times shows that route 6 is the fastest and requires the least amount of ΔV in order to reach Jupiter. To reach Saturn, route 5 is best compared to the other routes to Saturn: they take longer or require more ΔV. Again, route 5 and 6 perform best. One must note that while those routes have the lowest transfer times and lowest required ΔV, they can only use one planet for a gravity assist. Routes 1 to 4 benefit from two or more gravity assists. Remarkable to note is that the transfer times to 200 AU contradict the 30 years requirement. The extra ΔV needed to reach 200 AU within 30 years is shown in Table 3.5.

Route	ΔV extra needed [km/s]	Total ΔV [km/s]
1: (Earth-Venus-Jupiter)	14.49	26.07
2: (Earth-Venus-Saturn)	15.97	28.59
3: (Earth-Venus-Jupiter-Saturn)	6.69	35.67
4: (Earth-Jupiter-Saturn)	13.22	36.92
5: (Earth-Saturn)	21.03	28.32
6: (Earth-Jupiter)	20	26.36

Table 3.5: extra ΔV and total ΔV needed to reach 200 AU from the final planet (30 year requirement)

Utilising both results presented in Table 3.4 and Table 3.5 the routes can be compared in terms of total ΔV needed for the complete route. This is shown in Appendix A and in Figure A.1, Figure A.2, and Figure A.3. Results are also shown for a transfer time of 40 and 50 years. These plots show that route 1 and 6 perform the best, indicating a route utilising Jupiter and Venus as planets for the gravity

assists is preferred. It can be seen that the total ΔV needed from the propulsion subsystem ranges from 25 km/s up to around 35 km/s. This can be decreased by stretching the transfer time from 30 to 40 or even 50 years. The total ΔV for routes 1 and 6 will then change from around 26 km/s to 18.5 km/s or 14 km/s. This means for more detailed designs a balance must be found between the ΔV that can be provided and the time of travel. To improve this analysis and come up with a more feasible design/concept, the Hohmann transfer assumption should be relaxed and different transfers should also be analysed. The current analysis did not allow for more intricate routes and transfers. A good place to start a more intricate analysis is by utilising NASA's trajectory browser [9]. chapter 4 will go further into detail regarding the implications the results from the orbit analysis will have for the concepts for propulsion systems.

4

Propulsion

Prepared by Isabelle Joosten and proof-read by Jelle van der Meer

The following chapter lists and describes the different concepts considered in the design of the Heliosphere Probe's propulsion system. Although the launcher is responsible for bringing the probe into an Earth escape trajectory, the probe's onboard propulsion system ensures it can reach the desired 200 AU within 30 years. At the time of writing this report, the exact propulsion method is still uncertain, as it appears not a single propulsion method considered satisfies all requirements as set by the client (see chapter 2). This chapter nevertheless aims to give an as complete as possible overview of the current design state.

4.1. Influence of other subsystems

The preliminary design of the propulsion system is heavily influenced by the orbit design (see chapter 3), and, especially when electric propulsion is considered, the electrical subsystem (see chapter 9). Whichever method is used, the sizing of the propulsion system is driven by the required ΔV. For chemical and electric propulsion, the ΔV in m/s follows from the Tsiolkovsky equation:

$$\Delta V = v_{eq} * \ln \frac{m_o}{m_o - m_p} \tag{4.1}$$

in which v_{eq} denotes the equivalent jet velocity, m_o the initial spacecraft mass, and m_p the propellant mass. The required ΔV is a characteristic of the trajectory chosen, while the jet velocity is a characteristic of the thruster itself. Thus, when (approximate) numbers for these values are known, the fraction of the total mass that will need to be allocated to propellant can be estimated.

4.2. Electrostatic propulsion

Initially, an electrostatic propulsion system was considered. Electrostatic thrusters tend to generate low thrust but have a relatively high jet velocity, making them a good fit for long distance missions, as they are capable of efficiently providing low but constant thrust for longer periods. They work by ionising a propellant and accelerating these ions in an electric field before emitting them. This emission is what provides the thrust.
The jet velocity is given by the following equation:

$$v_e = \sqrt{\frac{2eN_AV}{M_W}} \tag{4.2}$$

where e is the charge of a single electron ($1.60221 * 10^{-19}$ Coulomb), N_A is Avogadro's number ($6.0221 * 10^{23}$ mol^{-1}), V is the grid voltage in Volt, and M_W is the molecular mass of the propellant in kg/mol. The grid voltage is typically in the range of 1000-2000 Volt, and for the purpose of this analysis the conservative value of 1000 Volt is used. By combining Equation 4.1 and Equation 4.2, the propellant mass required can be estimated. From Figure A.1 it follows that the trajectory with the smallest total

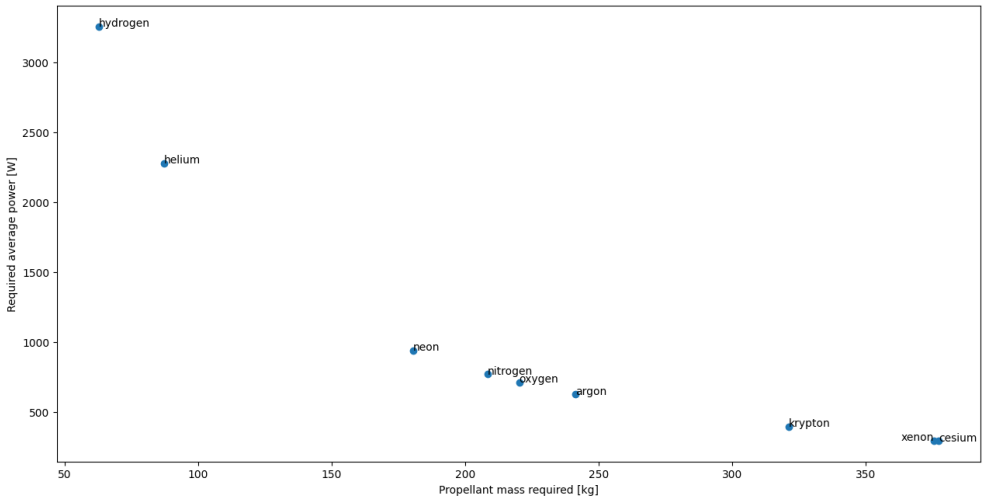

Figure 4.1: The minimum propellant mass and power required to reach 200 AU within 30 years, plotted for different possible electrostatic thruster propellants.

ΔV required is route 1 with a ΔV of 26.07 km/s. The average mass flow can be found simply by dividing the propellant mass by the total flight time. The thruster efficiency is given by the following equation:

$$\eta = \frac{P_e}{0.5 \frac{M_W}{N_A} v_e^2 + e_I + e_L} \tag{4.3}$$

where P_e is the exhaust power in watt, e_I is the ionisation potential of the fuel used in Joules, and e_L is the energy loss in Joules. The energy loss is generally in the range of 50-100 eV, and for this analysis the conservative value of 50 eV is used. The required power then follows by dividing the exhaust power by the thruster efficiency. Using a python script, a number of possible propellants were compared in terms of mass and power required, assuming an initial spacecraft mass of 250 kg. The results are summarised in Figure 4.1. There appears to be an inverse correlation between mass and power required. The propellant with the lowest power requirement, cesium, requires 208 watts, which already exceeds the total power budget. It also requires 270 kg of propellant, exceeding the probe's assumed total initial mass. The propellant with the lowest mass requirement, hydrogen, requires only 44.9 kg, which could be feasible, however it also requires 2325 watts in power. Assuming a more efficient thruster (e.g. with a grid voltage of 2000 Volt and only 50 eV of energy loss) does not make a significant difference. It can be concluded that, in its present form and based on the probe's current trajectory design, electrostatic propulsion is not a feasible solution. It should be noted, though, that by disregarding the 30 year requirement for the travel time and increasing it to 40 or even 50 years, the required ΔV and thus the required propellant mass and power all decrease. However, using the same calculation steps as for 30 years, and after discussing the matter with the mission client, it was concluded that the decrease in mass and power was not worth the increase in travel time.

4.3. Chemical propulsion

Chemical propulsion was briefly considered as an alternative to electrostatic propulsion as it would require a significantly lower power budget. However, assuming an approximate equivalent jet velocity of 450 (typical for liquid oxygen and liquid hydrogen thrusters[1]), solving Equation 4.1 leads to a propellant mass/initial mass ratio of 99.7%. Such a high ratio means that chemical propulsion is also not a feasible solution.

[1] from: `https://en.wikipedia.org/w/index.php?title=Specific_impulse&oldid=1188438364`, accessed on 09/01/2024

4.4. Solar sails

Initially in this analysis, solar sails were not considered as propulsion system due to their TRL: as of 2022, no aspect of solar sail technology has a TRL higher than 4[10], meaning this solution would not satisfy the requirement for minimum TRL as stated in chapter 2. However, as the other options considered turned out not to be feasible, solar sails were reconsidered after it was discussed with the mission client. Due to time constraints, the solar sail concept is not worked out in as much detail as the previously discussed ones, but based on literature it appears promising. In the 2007 ESA proposal[11] for a heliosphere probe, a 246 meter wide square solar sail is shown to be capable of accelerating a 467 kg probe to a velocity sufficient to reach 200 AU within 27 years. In another proposal, published by NASA in 2000, a hexagonal sail with a diameter of 400 meters is selected to propel a 150 kg probe to 200 AU in only 15 years[12]. These results imply a solar sail would satisfy all mission requirements except the TRL requirement. Thus, investing in extensive solar sail research and testing is necessary to fulfil this mission.

The mass of the propulsion system is estimated to be around 250 kg when compared to that in [11]. This would result in a price of around 14.5 million euro [13] (see figure **??** in appendix **??**). This is a very rough approximation for the price since the actual prices are hard to find for solar sail technology due to the novelty and low TRL of the design. These results are summarized in table 4.1.

	Margin	**Value**
Cost	-	14.5M €
Mass	-	250kg
Power	-	0 W

Table 4.1: Cost and mass budgets for the propulsion subsystem

5

Attitude Determination and Control

Prepared by Samuel van Erk and proof-read by Finn Heijink

The determination and control of the orientation and rotation of the spacecraft is handled by the Attitude Determination and Control subsystem (ADCS).

5.1. Requirements

The ESA study [11] mentions a 0.5° pointing accuracy. Our communication subsystem requires a pointing accuracy of 0.2°. New Horizons [14][15] and the Johns Hopkins Interstellar Probe (JHIP) [16] require a similar pointing of 0.2°. Thus, we take inspiration from their ADCS systems.

5.2. Attitude Determination

In the ESA study, attitude determination is achieved using two star trackers in combination with Micro-Electro-Mechanical System (MEMS) gyroscopes. New Horizons and the JHIP use two star trackers, Inertial Measurement Units (IMUs) and a sun sensor. We decided on two star trackers, two gyroscopes and a sun sensor. The sun sensor is added to provide extra safety in case the spacecraft loses inertial attitude knowledge, or its position with respect to Earth [16]. We use gyroscopes instead of IMUs since European missions still rely on American IMUs [17]. The European IMUs that are currently being developed have no flight heritage. Thus, we favour using gyroscopes, like the ESA paper suggested [11].

5.2.1. Star trackers

For the star trackers, the AA-STR star trackers by the European company Leonardo will be used [18]. This is a more advanced version of the A-STR star tracker, which was used by New Horizons and the JHIP also planned on using [14][16]. The AA-STR performs similarly to the A-STR and has reduced weight, power and cost. Since it also has a good flight heritage, this is a great fit for our mission. The A-STR star trackers that were used by New Horizons were redesigned to use time-delayed integration techniques to provide autonomous spacecraft attitude estimates at 10 Hz at spin rates up to 10 rpm[14]. Since our spacecraft will be spinning as well, such a redesign might be necessary.

5.2.2. Sun sensor

As stated before, the sun sensor is used for extra safety. New Horizons uses the Digital Sun Sensor (DSS) by the NH from the American company Adcole [19]. We use a European alternative, the Smart Sun Sensor (S3) by Leonardo. This sensor has an accuracy of 0.02°, which is much better than the 0.1° from the DSS [19][20]. It is limited to a distance of 50 AU from the Sun, which means that it can only be used at the beginning of the mission. However, after 50 AU, the influence of the Sun and planetary bodies is minimal, which results in a low likelihood that the sun sensor is necessary [11].

5.2.3. Gyroscope

The ESA paper talks about using MEMS gyroscopes, which is attractive for our mission because of their small mass, size, and low power consumption [21][22]. The only MEMS gyroscope space flight heritage is on the CryoSAT-2, which has a three-year lifetime [23]. There is no flight heritage for deep space MEMS. Besides, the MEMS gyroscopes have an Angular Random Walk (ARW) of 0.15°/h [23][24], which is significantly larger than the 0.005°/h of the IMU used by New Horizons [25]. Thus, we decided on using the Astrix 90 Fiber Optic Gyroscopes (FOG) instead, which have 0.005°/h accuracy, are qualified for deep space missions and have sufficient flight heritage [26].

5.3. Attitude Control

To control the orientation of the spacecraft, periodically thrusters are used to align the spacecraft. ESA proposes six Indium Field Emission Electric Propulsion (FEEP) thrusters, since these have high specific impulse, thus requiring less propellant mass than e.g. hydrazine thrusters[15]. Their small thrust is not considered a problem, since attitude disturbances are small due to the large distance from the Sun and other planetary bodies[11]. The three main disadvantages that ESA mentions concerning FEEP thrusters are limited flight heritage, limited lifetime tests and possible contamination of the payload by the thruster plume [11]. The European company ENPULSION produces FEEP thrusters of which more than 100 units have been launched. Thus, the flight heritage of FEEP thrusters has increased and further flight heritage can be expected. The same company has an ongoing thruster lifetime test which has demonstrated more than 20,000 h of firing without degradation of the emitter performance [27]. The third disadvantage, possible contamination, as well as possible degradation of the spacecraft body by emitted droplets [28] must still be assessed. We will use the ENPULSION NANO R^3 [29] since this provides the best radiation shielding.

For a robust and stable attitude, the spacecraft is spin-stabilized after the jettison of the solar sail. The spacecraft will spin around the axis of the antenna with a spin rate between 1 and 3 rpm.

5.4. Budgets

5.4.1. Mass

The mass of the individual star trackers is 2.6 kg, and the gyroscope weighs 4.5 kg. We use two star trackers and gyroscopes for redundancy. The sun sensor weighs 0.33 kg, the thrusters weigh 1.1 kg and use 0.3 kg of propellant each. As stated, six thrusters are used. This brings the total mass up to 22.9 kg. We include a margin of 20%, which gives a mass of 27.5 kg

5.4.2. Power

The star trackers consume 5.6 W at T=20 °C, 12.6 W at T=60 °C, the sun sensor uses 1 W, the gyroscopes use 13,5 W and the thrusters use 15 W. The star trackers will not be on when a correction manoeuvre is done. To limit the peak power usage only one thruster will be used at a time [14].
This means that the peak power is given by the gyroscope power (13.5 W) and the thruster power (15 W), which gives 18.5 W. Again, we include a margin of 20%, which results in a peak power of 34.2 W.

5.4.3. Cost

For the star trackers, we could not find a price, so we used €1M, which is listed as the price for very expensive and ultra-accurate star trackers [30]. For the sun sensor, we estimated a maximum price of €100,000. A less shielded, but comparable version of the thruster costs €38,400 [27]. If we double that, we get a price of €460,800 for all thrusters. The total propellant costs approximately €1,000. For the gyroscopes, we use a budget of €1M as well. This leads to a maximum hardware price of €3.5M. The production costs are estimated using The New SMAD [13], which, after correcting for inflation and currency conversion yields recurring costs of €14.8M and recurring costs of €8.5M. This brings the total cost to €26.7M.

	Margin	Value
Cost	-	<28M €
Mass	20%	27.5kg
Power	20%	35 W

Table 5.1: Cost, mass and power budgets for the attitude determination and control subsystem

6

Telemetry, Tracking and Control

Prepared by Raul Cotar and proof-read by Fanni Fiedrich

6.1. Introduction

The telemetry, tracking and command subsystems is tasked with providing a reliable data connection with Earth as well as providing ranging information. Radio telecommunication is regarded as a major challenge of the mission concept design due to the tight power budget and large transmission range.

6.2. Requirements

Requirement	Value	Note
Downlink @ 7AU	1000bps	Minimum requested by client
Downlink @ 200AU	200bps	Minimum requested by client
Uplink @ 200AU	5bps	Minimum requested by client
Power budget	62.5W	Maximum power in downlink windows
Reflector diameter	4.5m	Limited by launcher fairing diameter

Table 6.1: Mission Requirements

The requirements for this subsystem have been derived from the ESA IHP[11] mission concept and adjusted for the changes in launcher capabilities and the limitations of the other subsystems, predominantly power generation and distribution. The main requirement is to have a downlink data rate sufficient for the scientific data collection goals and uplink rate sufficient for spacecraft management and diagnosis. Furthermore, the power and mass requirements of the subsystem should be minimized. The exact values are shown in Table 6.1.

6.3. Design considerations and tradeoffs

Radio frequencies in the X, Ku and Ka bands, as well as optical (LASER) solutions have been considered. While optical systems have significant theoretical advantages over normal radio waves in terms of data rates, they do not meet the TRL requirements of the project and would further increase the complexity and cost of the subsystem, especially when also considering ground stations. The choice then remains between the different radio bands. Both ESA's Estrack and NASA's Deep Space Network (DSN) are focusing their developments on the Ka-band for its larger bandwidth and data rate potential, while at the moment the X-band is the more widely supported one due to its more extensive heritage [31]. The other most important difference between the two is atmosphere attenuation: the Ka-band has much worse transmissivity through Earth's atmosphere and is especially affected by rain.[32] In the end, the RF band of choice in this proposal is the Ka-band due to its better bandwidth potential, antenna gain characteristics and future support.

Band	Uplink frequency	Downlink frequency	Max Downlink Bandwidth	Notes
X	7.145 – 7.190 GHz	8.400 – 8.450 GHz	5 MHz	lower gain, higher power
Ka	34.200 – 34.700 GHz	31.800 – 32.300 GHz	50 MHz	high noise and attenuation

Table 6.2: RF Band Comparison

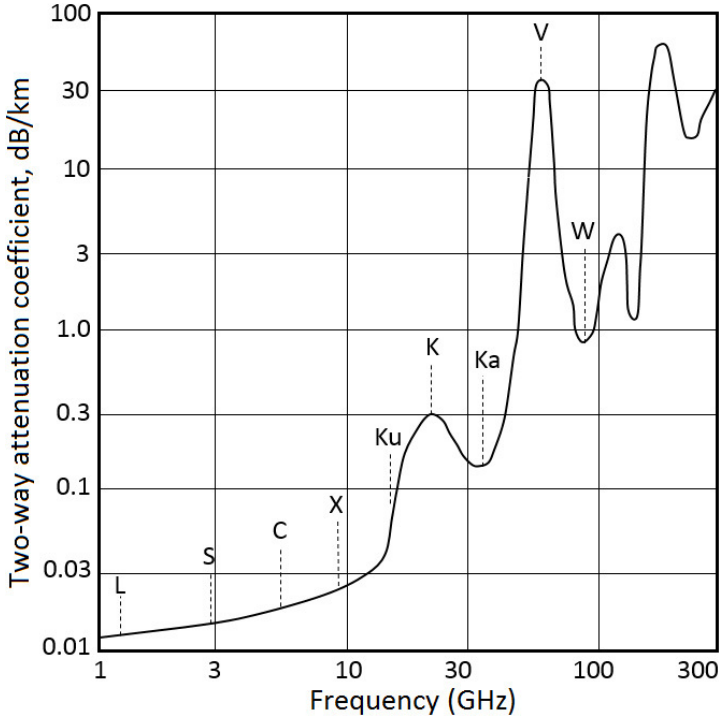

Figure 6.1: Atmosphere attenuation by frequency [32]

The main issues that have to be dealt with are system noise temperature and atmospheric attenuation. The former can be mitigated with small advancement in antenna feed, low-noise amplifier (LNA) and receiver technology, that are already ongoing at Estrack[33]. Ground stations are constantly improving since they are used by virtually all space missions, and so are of common interest. We think that with small incremental updates over the existing hardware, there should not be any significant problem in using the existing ones for our mission. They key areas of improvement we have identified are: pointing accuracy, aperture efficiency and system noise temperature.

Another possible solution that might be worth looking into is using a relay satellite close to Earth (GEO/L2) that would receive the signal from the our spacecraft and re-transmit it down to Earth. Especially in a geostationary orbit, this satellite could double as a regular telecommunication satellite thus lowering the overall costs. The great advantage of this approach is that the first hop does not pass through the atmosphere anymore and thus considerably higher data rates could be possible. The second hop will also be using solar powered (and thus more powerful) radios and over a much smaller distance. The receive antenna would still need to be large, but deployable mesh antennas are becoming better and better so that should pose little problem.[34]

Since the science data rate is around 70-270bps raw and around 67bps after compression (assuming 200bps with a compression ratio of 3), downlinking all the gathered data may not be feasible. Data transmission is a recurring cost since ground stations need to be allocated for every transmission window. In the interest of keeping costs low and not occupying the ground stations too much we have decided upon a schedule of weekly/bi-weekly 10-hour-long transmission windows that can be adjusted based on the value of the provided data and future economic factors. A system could be put in place, where a ”filter” is applied to the data that gets downlinked - a specified selection of telemetry and payload-generated data that can be modified with commands from ground. This way, the most rele-

vant data can be chosen dynamically ahead of time for each transmission window.

6.4. Final design proposal

Parameter	Value	Notes
Reflector diameter	3.7 m	carbon fibre construction
3dB Full beam width	0.15°	nominal
Gain	61dBi	aperture efficiency 83%[34]
Total power	62.5 W	
Radiated power	56.5 W	
Nominal downlink frequency	32050 MHz	Ka-band downlink standard
Nominal uplink frequency	34450 MHz	Ka-band uplink standard

Table 6.3: HGA Specifications

We have settled on a pair of redundant Ka-band radios with a 3.7m Cassegrain high gain antenna (HGA) and 3 small low gain antennas (LGA) spread around the spacecraft to allow for omni-directional coverage during early mission stages. Deployable antennas and mesh reflectors have also been considered, but voted against due to their increased risk of deformation and destabilization, increased complexity and higher costs.

The HGA is of particular interest since it is the primary antenna of the spacecraft. Its properties can be seen in Table 6.3. Like the ESA IHP[31] study, our study also proposes to incorporate a piezo-controlled deformable secondary reflector. This enables the main lobe to be steered by as much as 2° (estimated) to increase pointing accuracy, and can also be used to temporarily increase the the beam width when close to Earth to ease off the otherwise stringent pointing requirements. This device is the reason for the extremely lenient stated pointing requirement of <0.2°. In reality, the ADCS system offers much better accuracy compared to the requirement (in the order of milliarcseconds). The deformable secondary reflector is one of the few areas of the TT&C subsystem that need significant developments since the TRL level is low and the entire HGA is dependant on its performance.

The HGA, LNA and receiver will be thermally decoupled from the rest of the spacecraft in order to lower the noise temperature.

The only 2 ground station networks capable of communicating with the spacecraft in the later stages of the mission are ESA's Estrack and NASA's DSN. We will focus on Estrack for the calculations, but note that the DSN is similarly capable (even more so) so infrastructure sharing can definitely be taken into account when planning downlink windows. We also assume small improvements to the 35-meter DSS network, allowing individual antennas to reach a gain of 80dBi in the downlink Ka-band and a 30K system noise temperature; the actual values seem to be around 79dBi and 35-45K in the present. These improvements would also be beneficial to other future ESA mission that utilise the Ka-band.

6.5. Link budget calculation

Unlike the ESA IHP study[31], we have chosen to increase the reflector size and power budget to allow the use frequency/phase modulation as opposed to pulse-position modulation (PPM). This allows us to use already existing infrastructure while also possibly providing better data rates than PPM. In the end we concluded that a bitrate of 270 bps should be achievable at the mission goal of 200 AU. When we first switch to the HGA at around 2 AU (1 AU from Earth) the bitrate will vastly exceed the requirement, but due to time constraints we did not investigate the communications using the 3 LGAs. However, low-gain antennas close to Earth have vast flight heritage and so the analysis should not pose any difficulties.

Parameter	Value	Notes
DSS System Noise Temperature	30 K	estimation[35]
Pointing Error	<0.1 bB	estimation[35]
Atmosphere Attenuation	1.53 dB	95%weather conditions [36]
Link Margin	3.5 dB	
Received Signal Power	-145.16 dBm	
Noise Power	-151.16 dBm	
SNR	6.00 dBm	downlink
Modulation	QPSK	0.99 bits/symbol
Coding	Turbo code r=1/2	
Coding Gain	9.8 dB	
Bit Rate	24.3 dB	**270 bps**
Bandwidth	270 Hz	

Table 6.4: Downlink budget at 200 AU

6.6. Mass Budget

Component	Count	Unit mass (kg)	Subtotal (kg)	20% margin (kg)
HGA	1	26	26	5.2
LGA	3	1	3	0.6
radio	2	2.5	5	1
wires	-	2	2	0.4
TOTAL	-	-	36	7.2

Table 6.5: RF Band Comparison

6.7. Final Thoughts

The TT&C subsystem poses challenges, but it is definitely feasible, even using high TRL components. Data rates slightly exceeding the requirements are possible and give some room for ranging and telemetry data to be transmitted. Further research into the space-based relay could be worth it since it has the possibility to significantly increase data rates and allow the mission life time to be extended without loosing so much scientific data.

	Margin	**Value**
Cost	-	28M €
Mass	20%	43.2 kg
Power (transmission peak)	-	62.5 W
Power (weekly average)	-	3.72 W
Power (biweekly average)	-	1.86 W

Table 6.6: Cost, mass and power budgets for the TT&C subsystem

7

Structures and Mechanisms

Prepared by Iorcan Jagt and proof-read by Huub Reitsma

This chapter will explain the structure. First it will give information on the primary structure. Afterwards more information on the secondary structures will be provided.

7.1. Primary structure

The probes main structure has a 1 m diameter and 1 m long load bearing cylinder as a base. Inside the cylinder is a honeycomb frame giving extra strength and better mounting points for the different components. The cylinder has on one side the antenna mounted and on the other side the propulsion. On the propulsion side an extra deck is constructed so that the Radio-Thermal Generators aren't too close to the probe. Different views on a CAD model of the primary structure can be seen in Appendix E.

The material chosen for the whole structure is Aluminium Alloy 5052. Alloy 5052 is a stronger alloy of aluminium, is on the cheaper side compared to other frequently used space faring materials and gives good protection against radiation. This material was chosen via a trade off table which compared 5 materials with each other. Information on the materials was found in a material database called Granta Edupack. The materials compared are: Aluminium Alloy 2024, Aluminium Alloy 5052, Beryllium-aluminum Alloy, Titanium and Carbon Fibre. The complete trade off table can be seen in Table 7.1. Four criteria were chosen to determine the best material: Cost, Density, Strength and Corrosion Resistance. Aluminium Alloy 5052 was chosen over Aluminium Alloy 2024 because it was a bit cheaper.

The maximum loads on the probe will be experienced during launch. Because a requirement states that only Ariana 62, Ariana 64 or Vega-E can be used to launch the probe, the choice for launcher is limited. For the Vesta-E no loads can be found for the public. On the other hand the user manual for the Ariana 62 and 64 can be found online [37].
The manual states that in lateral direction the natural frequency needs to be higher than 6 HZ and the loads experienced would be a maximum of 2g. In the longitudinal direction the frequency needs to be higher than 20 Hz and the loads will not exceed 6g. By multiplying the values with the 1.25 safety factors and using the thin wall assumptions the necessary thickness could be calculated. The minimum thickness needed is 0.2 mm. Finally because of the high radiation the probe will experience, the actual thickness will be 10 times bigger and additional lead foil can be applied.

Material	Cost	Density	Strength	Corrosion Ressistance	Total
Aluminium Alloy 2024	3	3	2	3	0.6875
Aluminium Alloy 5052	3	3	2	3	0.6875
Beryllium-aluminum Alloy	1	3	3	3	0.625
Titanium	2	2	3	3	0.625
Carbon Fibre	2	3	1	3	0.5625

Table 7.1: The trade off table for which material should be used. The first column contains all the materials. The top row contains the criteria. Each material is given a grade of 1 (bad), 2 (okay) or 3 (great). Then the average was calculated which is shown in the last column

7.2. Extras

For some of the instruments onboard booms are necessary. The deployable CFRP boom from DRL has chosen for this probe design. This is a lightweight and low storage needed boom. One boom being of 10 m will be onboard. Alternatives would be to use telescopic masts or Nasas Deployable Composite Boom. Apart from the main boom, two wire probe antennas of 15 m will be onboard for the plasma wave analyser. Extra wire booms will be used for a spinning deployment mechanism of the solar sail. Finally for the solar sail jettison, the propulsion and the main structure will be connected with a marman clamp which is secured with two explosive bolts. Instead of a marman clamp a motorized lightband from rocketlab could be used. Calculations for the cost, mass and power can be seen in Appendix E.

	Margin	**Value**
Cost	-	~~1~~4M €
Mass	20%	106.8kg
Power	20%	40W

Table 7.2: Cost, mass and power budgets for the structures subsystem.

8

Thermal control

Prepared by Huub Reitsma and proof-read by Samuel van Erk

The thermal control subsystem aims to provide adequate temperatures to ensure operational temperatures for the instruments and other components of the spacecraft. The design of this subsystem is driven by the most extreme case, where the spacecraft is at 200 AU. The reason for this is that in this case the spacecraft is the farthest from the sun and therefore the most extreme temperatures take place here. Because the electrical power is severely limited due to the large distance from the Sun, and thus not having the ability to use the Sun for electrical power, a passive approach was taken to the thermal control. This approach was to ensure the reliability of the thermal control subsystem as there is a lack of moving parts.

Because of the extreme distances the system, thermally, does not change much. Because of this, a steady-state approach analysis can be taken which simplifies the analysis. By wrapping most of the spacecraft in multi-layer insulation (MLI) the spacecraft can retain most of the heat. Part of the heating necessary for keeping an operational temperature range is done by dissipation of the payload and other various components that require power. The rest of the heating necessary can be gained by using the waste heat from the radioisotope thermoelectric generators, or RTGs. By collecting a total of around 6% of waste heat from the end-of-life RTG, enough heat is added to the system to keep the temperature of the spacecraft within the operational range of -10 °C to 40 °C at 200 AU. In the beginning, there is a small window where the temperature could be slightly above 40 °C but this would be within the survivable non-operational range of -20 °C to 50 °C.

8.1. Components of the subsystem

As is said before the thermal control subsystem is completely passive and thus does not require any electrical power from the RTGs. The waste heat of the RTGs, as stated above, is used, so the RTGs have to be thermally coupled to provide around 6% of the waste heat they produce. Besides this, the spacecraft would be almost fully wrapped in multi-layer insulation. This would ensure that the spacecraft would retain the heat from the dissipation of the instruments. The requirements for this MLI would be an emissivity coefficient of 0.05 which is on the high end of known MLI as most MLI have a better emissivity coefficient, that being a lower emissivity coefficient [38]. MLI with a better emissivity coefficient would mean that less waste heat from the RTGs is needed to sustain the said operational temperature range. With these components, no radiators are needed as the main objective of this system is to retain as much heat as possible and radiators would be counterproductive to this. Moreover, reflector shields would be mounted on the RTGs to counteract overheating of the spacecraft and additionally, it would protect against any harmful radiation the RTGs might produce. Additionally, the antenna is thermally decoupled from the rest of the spacecraft to reduce the amount of surface area. This also helps to prevent overheating from the Sun as the antenna is pointing at the Earth and thus also in the general vicinity of the Sun. This prevents the heat from the Sun from coming into the spacecraft and potentially damaging the payload or other components. Lastly, if other routes are taken, for example,

a gravity assist using the Sun, then extra measures have to be taken to ensure the thermal ranges of the spacecraft such as a Sun shield.

For the overall budget and mass estimations of the thermal subsystem, the reader is referred to Table 8.1, and for the in-depth calculations for these numbers, one can look at Appendix D.

	Margin	**Value**
Cost	-	4.2M €
Mass	20%	18kg
Power	-	0

Table 8.1: Cost, mass and power budgets for the thermal subsystem.

9

Electrical Power

Prepared by Finn Heijink and proof-read by Iorcan Jagt

9.1. Introduction

The electrical power subsystem is tasked with the handling of electrical power throughout the spacecraft. Since the spacecraft is travelling far away from the sun, solar power is hard to use: since the solar flux decreases quadratically as the distance from the sun increases, alternatives must be found. A popular alternative for solar power is a Radio-thermal Generator (RTG): by using the heat created from the decay of radioactive particles to generate electricity, no solar power is needed. The drawback of this source is the risks and dangers of using nuclear fuel and the high cost. Different RTG designs will be compared and the total cost, weight and generated power of the system will be provided. For more detailed calculations of the subsystem, see Appendix F.

9.2. Power budget and requirements

It is important that the power system is able to produce enough power for all parts of the mission: the peak power during every stage of the mission should be produced (at least) since the RTG can not increase the power output; it will produce a continuous (degrading) outflow of power. To find this peak power, a power budget is created: the average and peak power usage by each subsystem of the spacecraft is noted to find the average and peak power of the entire spacecraft. The power budget is given in Figure 9.1. Note that the after the deployment of the solar sail the maximum power needed is 128.4 W since the deployment actuators are not needed anymore, while before that a maximum power of 155.4 W is needed.

It is also important that the subsystem lasts for the designated time of around 30 years. Since the nuclear fuel decreases in mass due to the decay and the thermo-electric converters decrease in efficiency over time, the End-of-Life (EOL) power must be high enough such that all operations that occur around this time can be performed. The numerical requirements related to this are found in Appendix F.

9.3. RTG Design and Specifications

When it comes to RTGs, ESA is very limited in options: no European RTG has ever flown in space, and the current research being done by ESA has a focus on using Americium-241 as a source of nuclear fuel [39]. Since Americium-241 systems have a way lower specific power (power generated per kilogram of the RTG system) than the RTGs used by NASA, [39] [40] [41] the choice was made to use American technology instead of European technology. This is worked out numerically in Appendix F.

To keep the mass and Beginning-of-Life (BOL) power as low as possible for thermal reasons, we need to look for a RTG with a low system decay and a high specific power. It turns out that the New MMRTG design by NASA performs the best in this regard, with a specific power of 4.375 watts of electrical power per kilogram, a Technology Readiness Level (TRL) of 7 and a half-life of around 53.54 years,

Subsystem		Spacecraft recovery	Sail deployment	Solar sailing	Science mode	Telecom mode
Payload	Average	16.0 W	0.0 W	3.0 W	16.0 W	0.0 W
	Peak	16.0 W	0.0 W	3.0 W	16.0 W	0.0 W
ADCS	Average	17.5 W	17.5 W	20 W	17.5 W	17.5 W
	Peak	28.5 W	28.5 W	28.5 W	28.5 W	28.5 W
Telecom	Average	2.7 W	1.2 W	2.7 W	2.7 W	3.8 W
	Peak	45.0 W	20.0 W	45.0 W	45.0 W	62.5 W
OBDH	Average	15.0 W	15.0 W	15.0 W	15.0 W	15.0 W
	Peak	15.0 W	15.0 W	15.0 W	15.0 W	15.0 W
Power supply	Average	1.0 W	1.0 W	1.0 W	1.0 W	1.0 W
	Peak	1.0 W	1.0 W	1.0 W	1.0 W	1.0 W
Thermal Control	Average	0.0 W	0.0 W	0.0 W	0.0 W	0.0 W
	Peak	0.0 W	0.0 W	0.0 W	0.0 W	0.0 W
Deployment actuators	Average	0.0 W	40.0 W	0.0 W	0.0 W	0.0 W
	Peak	0.0 W	65.0 W	0.0 W	0.0 W	0.0 W
Subtotal	Average	52.2 W	74.7 W	41.7 W	52.2 W	37.3 W
	Peak	105.5 W	129.5 W	92.5 W	105.5 W	107 W
Incl. 20% margin	Average	60.8 W	88.8 W	48.2 W	60.8 W	44.8 W
	Peak	126.6 W	155.4 W	111 W	126.6 W	128.4 W

Figure 9.1: Power budget for the separate parts of the mission based on [11]

which equals a decay of around 1.29 percent per year [40]. For comparison, a European system using Americium-241 would have a specific power of around 2 watts of electrical power per kilogram and a decay of around 1.01% per year, with a TRL level of 5 [39]. If we want to fit the requirements such that we can power the spacecraft at all times using Figure 9.1, we need a RTG mass of 43.47 kg if we use NASA technology or 87.5 kg if we use ESA technology.

To get the final weight of the electrical power system, we also include the weight of the power electronics and a margin of 20%. The power electronics and routing system is based on the one used in [11] with a weight of 6 kg. Using this information, we obtain a total weight of around 60 kg for the total subsystem. We split the RTGs into two equal units such that the spin-balance of the spacecraft is better (as seen in [11]). We then assume the costs offered in [40] as a price per kilogram of the system, which is 0.71 million euro for a kilogram of RTG mass. This gives a final price for the RTG system of around 42.8 million euro. Since we include the price of the power electronics and routing as that of the RTG system per kilogram, we will likely overestimate the budget this way: the actual price will likely lie lower. We use this fact as another margin. With that, the final specifications of the electrical power subsystem are given in Table 9.1.

	Margin	**Value**
Cost	-	42.8M €
Mass	20%	60kg
Power (generated)	-	190.2W
Power (needed)	20%	1.2W

Table 9.1: Cost, mass and power budgets for the electrical power subsystem

10

Command and Data Handling

Prepared by Fanni Fiedrich and proof-read by Jelle van der Meer

The Command and Data Handling (C&DH) subsystem is a central subsystem responsible for controlling the spacecraft and handling on-board generated as well as up-linked data [42]. On-board generated data includes housekeeping data for monitoring the S/C health and the science data by the instruments. The design of the C&DH subsystem is driven by requirements further discussed in Appendix C. Overall, the goal is to increase reliability and decrease the power usage of the system. Radiation tolerance is also a major design consideration.

10.1. Subsystem Architecture

The C&DH subsystem is composed of systems on chips (SoCs), solid-state recorders (SSRs) and SpaceWire (SpW) routers connecting the components. A telemetry (TM) encoder as well as a telecommand (TC) decoder are integrated on the SoCs. The SoCs serve as the on-board computer (OBC) and are responsible for data processing and controls. The SSRs are the main memory for storing the on-board data. In the SpW network architecture, the SpW routing switches act as a connection between the components and forward the data packets [43], [44]. A simplified block diagram in Figure 10.1 displays the main components and the connections between them. The technologies used are similar to those outlined in the ESA study, while the architecture is based on the Johns Hopkins study [11], [16].

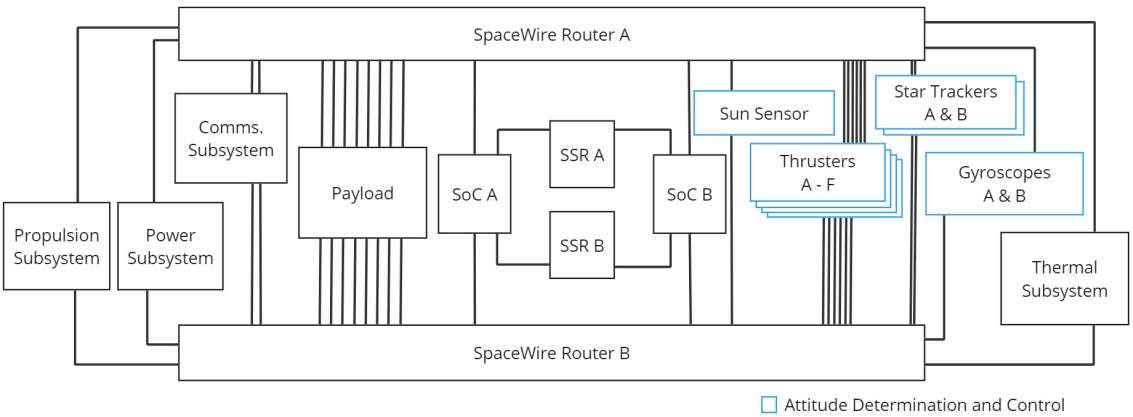

Figure 10.1: A simplified overview of the subsystem architecture and the connections to the other subsystems.

The system is designed to be dual-redundant to increase reliability and mitigate radiation impact.

Critical components, namely the SoC, the SSR and the routers, are duplicated. Each component and connection is cross-strapped across both routers, and the software re-configures the system to use the healthy components, if necessary [16]. Hot standby sparing is used for both the processors and routers. Therefore, one processor and router is powered fully, and the additional components are powered in stand-by mode [42]. This way, the redundant processor or router can be powered on more quickly if the primary one fails [15], [42]. To detect processor faults, a watchdog timer is used. The assumption for a watchdog timer is that a system does not have any faults, as long as the timer is reset in specified intervals [42]. Finally, all components are radiation hardened to mitigate radiation impact further [43], [45], [46].

A SpaceWire architecture is used, similar to the ESA study design [11]. The main reason is that it is developed by ESA, for ESA missions [47]. It is widely integrated also in non-European space missions and ESA encourages it's usage [48], [49]. It is a highly reliable point-to-point interface [47], [50]. A data rate of more than 100 Mbps is supported [44]. This is sufficiently high for the spacecraft needs. There is also European-developed technology available for suitable radiation-hardened SpW routers [43].

The payload instruments are connected individually to the SpW routers. The system does not include any remote interface unit or payload processor. The reason for this design choice is that the focus lays on decreasing complexity and power consumption. The data load by the payload is not high, so it is expected to be possible for the main processor to handle it.

10.2. Subsystem Components

The following subsections provide more detail into the subsystem component specifications.

10.2.1. Central Processor

The choice of the central processor is mainly determined by the radiation hardening factor, and the requirement to use EU technology. ESA has developed multiple versions of LEON-core microprocessors [51]. Here, a radiation hardened dual-core LEON3-FT 32-bit SoC is used [45]. Overall, a LEON-core processor is chosen over other OBCs since it is ESA-developed technology [51]. An additional reason is that the LEON3-FT microprocessor itself, as well as the specific dual-core processor have flight heritage [52], [53]. The processor in the referenced datasheet does not need to be the exact model used. However, it provides some insight into current technologies. For example, it supports error correction for the on-chip memories [45].

Generally, SoC offer higher integration and therefore have lower mass than a larger OBC. The SoC has two processors which makes it possible to save power by powering one core, if there are no high processing needs [16], [45].

10.2.2. Mass Memory

The main memory needs to be radiation-hardened non-volatile erasable memory to be able to store the science and S/C data. SSRs are used, as is also the case for the Johns Hopkins study and New Horizons mission [15], [16]. Different possibilities for memory types include SRAM, DRAM, Flash, MRAM, FERAM and CRAM/PCM [54]. Since it has to be non-volatile, SRAM, DRAM and Flash cannot be used. MRAM has a high radiation tolerance of generally up to 1 Mrad (TID) [54]. Even though it has a higher power usage than for example FeRAM, it is chosen here for its practically unlimited read/write endurance [54], [55]. There are options available for radiation hardened space-grade MRAM with suitable sizes [46].

In order to calculate the size of the storage, the amount of science data needs to be calculated. The payload has a data rate of 70 - 270 bps, with one measurement taken per hour. The longest interval throughout the mission is data transmission on a bi-weekly basis, as outlined in chapter 6.

For a mission stage with bi-weekly communication, consider a scenario in which something fails on the spacecraft, causing it to miss a transmission window. On the ground, an update to fix the spacecraft can then be prepared in following the two weeks up to the next window. Afterwards, it is transmitted to the spacecraft which then would need to reboot and run the fix. Only in the third window, the stored science data can then be transmitted again. This results in a worst-case accumulation of six weeks worth of science data. A more detailed calculation can be found in Appendix C. Including a margin of 50%, the worst-case amount of science data is given by 0.047628 to $0.183708\ GB$ [56]. A data compression factor of 3 is assumed for the transmission of data to the ground.

Additionally, the main memory stores the operating system, any needed command chains as well as telemetry and spacecraft health related data. Here, 4GB cards are proposed instead of the 2GB cards in the ESA study [11]. This allows for additional freedom, and makes it possible to store larger software. The storage can also be used to store data in a redundant manner. The data is divided into blocks on the memory card, and can be written in multiple locations redundantly. However, if at a later stage in the mission it is clear that much less memory is required, switching to 2GB cards does not make a large difference power, volume or mass wise.

10.3. Budget Summary

Table 10.1 provides an overview of the estimated budgets for the C&DH subsystem, including margins [56]. The cost estimate is given as 40M € (see Appendix C). The cost does not include the software.

The mass is estimated at approximately 9kg, similar to the ESA study [11]. This is because the system is on a similar scale as the ESA reference study. The main contributor to the mass are SpaceWire cables, and the total length is difficult to estimate. Processors, memory cards and routers have only a small volume and are expected to weigh a few grams [43], [45], [46].

	Margin	**Value**
Cost	-	40M €
Mass	20%	9kg
Power	20%	15W

Table 10.1: Cost, mass and power budgets for the C&DH subsystem.

11 Budgets

Prepared by Finn Heijink and proof-read by Fanni Fiedrich

11.1. Mass Budget

The mass budget is estimated in the chapters of the corresponding subsystems. The weight of each subsystem (including the payload mass which is found in [11]) and the total mass including margins is given in Table 11.1. We use standard ESA margins for the mass estimating budget [56].

Subsystem	Mass
Propulsion	250 kg
Attitude Determination and Control	27.5 kg
Telemetry, Tracking and Control	43.2 kg
Structures & Mechanisms	106.8 kg
Thermal control	18 kg
Electrical power	60 kg
Command and Data Handling	9 kg
Payload	21.4 kg
Total (including 20% margin)	643.1 kg

Table 11.1: Mass budget of the spacecraft

11.2. Power Budget

The power budget is more complex to calculate due to the different stages of the mission having fluctuating power requirements. To avoid confusion, the power budget is given in more detail in Table 9.1 in chapter 9.

11.3. Cost Budget

The SMAD book has a table for estimating (rough order-of-magnitude) prices for different parts of the spacecraft [13]. This is used to give a rough indication of the price of the mission. Also see **??** for the tables from [13].

If we assume that the formula given for the price of the payload in [13] holds in case of a design life above 150 months, we obtain a cost of around 43.1 million euro for the complete payload. Note that the TRL of the payload is only 2 [11], which plays a role in the cost calculations [13] (see **??**).

The launch cost is estimated to be around 115 million euro if using the Ariane 64 launcher [57].

The spacecraft bus cost (the total cost of all of the subsystems) is around 186.1 million euro. Using this; the integration, assembly and testing of the spacecraft is estimated to be 62.1 million euro, the program level is estimated to be around 42.5 million euro, and the aerospace ground equipment is estimated to be around 60.1 million euro [13] (see **??**). Since the SMAD book does not offer extra cost calculations that play a role for the mission concept design and most of the information about prices is not readily available online, the final cost will be estimated based on the found values. The TRL level of the subsystems is used to increase the cost if the TRL level is low according to [13] (see **??**). Note that the decrease of the cost due to a high TRL is not applied to serve as an extra margin in the estimation of the cost.

Subsystem	Cost	TRL	TRL-adjusted cost
Propulsion	14.5M €	3	29.1M €
Attitude Determination and Control	28M €	8	28M €
Telemetry, Tracking and Control	28M €	7	28M €
Structures & Mechanisms	14M €	9	14M €
Thermal control	4.2M €	9	4.2M €
Electrical power	42.8M €	7	42.8M €
Command and Data Handling	40M €	7	40M €
Payload	43.1M €	2	129.3M €
Launch cost	115M €	-	-
Integration, assembly and testing	62.1M €	-	-
Program level	42.5M €	-	-
Aerospace Ground Equipment	60.1M €	-	-
Total (using TRL-adjusted costs)	595.1M €	-	-

Table 11.2: Cost budget of the spacecraft in FY24 euro. The inflation rates are calculated using [58]

Having calculated the final price of the mission to be around 595.1 million Euro, the very strong assumptions and simplifications made in the estimation of the price make this number very unreliable. This number serves as a very rough indication of the price, and since it is well below the budget of 1 billion euro the possibility that the budget can be met for the spacecraft is not out of the question. Further research should be done to refine the cost estimate, which is also an effect of refining the subsystem designs itself.

12

Conclusion

Prepared by Iorcan Jagt and proof-read by Huub Reitsma

In conclusion, the following concept is constructed. During the designing process some requirements were deemed impossible. This being the sole use of European technology and the technical readiness level being higher than 5. Apart from these requirements all the other requirements should be met with the final design. The final design consists of an aluminium cylinder base which will be propelled with a solar sail. With the propulsion the spacecraft shall pass Jupiter. To stay on course 6 Field Emission Electric Propulsion thrusters will be used. While the spacecraft is getting further away from earth, a four meter diameter antenna will be used to keep contact. The energy for this will be provided by the Radio Thermal Generators which also will be providing heat to the spacecraft. With the use of Multi layer insulation the heat will be retained using a passive approach for thermal control. Telecommunications rates will be sufficient all the way out to the mission goal of 200 AU, using the Ka-band high gain antenna. Finally the command and data handling will use systems on chips, solid-state recorders and SpaceWire routers.

References

[1] C. Impey. “Have we made an object that could travel 1% the speed of light?” (2021), [Online]. Available: https://www.yahoo.com/news/made-object-could-travel-1-131118755.html?guccounter=1&guce_referrer=aHR0cHM6Ly90aW5leWUuY29tLw&guce_referrer_sig=AQAAACkN2ITSDctBCiC_9adRjTL4V8vBEX61JK0v9pPlCqw8V3Gi8kUEiL7xzq-qy1QIvSYL-m2CN7qBuJUOkofIE29sLqJhyy6lUHc4LC42mshc52hvS4oaNER5weTi-G9LeVy6bhhGE6U1PZfgfaV6PLLbO7Vapg4-FEHCBJIWTtwT (visited on 11/15/2021).

[2] Wikipedia. “Interstellar probe.” (2024), [Online]. Available: https://en.wikipedia.org/wiki/Interstellar_probe#:~:text=As%20of%202023%2C%20there%20are,have%20actually%20reached%20interstellar%20space (visited on 01/07/2024).

[3] NASA. “Voyager 2 trajectory.” (2023), [Online]. Available: https://science.nasa.gov/resource/voyager-2-trajectory-through-the-solar-system/ (visited on 12/14/2023).

[4] J. H. University. “The path to pluto and beyond.” (2023), [Online]. Available: https://pluto.jhuapl.edu/Mission/The-Path-to-Pluto-and-Beyond.php (visited on 12/14/2023).

[5] NASA. “Pioneer-10.” (2023), [Online]. Available: https://science.nasa.gov/mission/pioneer-10/ (visited on 12/14/2023).

[6] NASA. “Pioneer-11.” (2023), [Online]. Available: https://science.nasa.gov/mission/pioneer-11/ (visited on 12/14/2023).

[7] T. P. Today. “Galileo flight path.” (2023), [Online]. Available: https://www.theplanetstoday.com/galileo_flight_path.html (visited on 12/14/2023).

[8] NASA. “Cassini trajectory.” (2023), [Online]. Available: https://science.nasa.gov/resource/cassini-trajectory/ (visited on 12/14/2023).

[9] NASA. “Nasa ames research center trajectory browser.” (2023), [Online]. Available: https://trajbrowser.arc.nasa.gov/index.php (visited on 01/09/2024).

[10] P. ZHAO, C. WU, and Y. LI, “Design and application of solar sailing: A review on key technologies,” *Chinese Journal of Aeronautics*, vol. 36, pp. 125–144, 5 May 2023, ISSN: 1000-9361. DOI: 10.1016/J.CJA.2022.11.002.

[11] A. Lyngvi, M. van den Berg, and P. Falkner, “Study overview of the interstellar heliopause probe,” vol. SCI-A/2006/114/IHP, 3 2007.

[12] R. A. Mewaldt and P. C. Liewer, “An interstellar probe mission to the boundaries of the heliosphere and nearby interstellar space,” 2000. DOI: 10.2514/6.2000-5173.

[13] J. Wertz, D. Everett, and J. Puschell, *Space Mission Engineering: The NewSMAD*, 2nd ed. Hawthorne, CA: Microcosm Press, 2015.

[14] C. B. Hersman, G. D. Rogers, V. A. Mallder, *et al.*, “The new horizons spacecraft: Past performance, future potential,” *Johns Hopkins APL Technical Digest*, vol. 37, 1 2023. [Online]. Available: www.jhuapl.edu/techdigest.

[15] G. H. Fountain, D. Y. Kusnierkiewicz, C. B. Hersman, *et al.*, “The new horizons spacecraft,” *Space science reviews*, vol. 140, pp. 23–47, 2008.

[16] R. L. Mcnutt, M. V. Paul, P. C. Brandt, and J. D. Kinnison, “Humanity’s journey to interstellar space,” Dec. 2021, Study done by John Hopkins.

[17] *European imu for space navigation | eurisa | project | fact sheet | h2020 | cordis | european commission*. [Online]. Available: https://cordis.europa.eu/project/id/101004205.

[18] *Aastr | leonardo - electronics*. [Online]. Available: https://electronics.leonardo.com/en/products/aastr.

[19] *Dss | adcole maryland aerospace*. [Online]. Available: https://satcatalog.s3.amazonaws.com/components/359/SatCatalog_-_Adcole_Maryland_Aerospace_-_Digital_Sun_Sensor_-_Datasheet.pdf?lastmod=20210708050402.

[20] Leonardo, "Smart sun sensor,"

[21] W. A. Gill, I. Howard, I. Mazhar, and K. McKee, "A review of mems vibrating gyroscopes and their reliability issues in harsh environments," *Sensors 2022, Vol. 22, Page 7405*, vol. 22, p. 7405, 19 Sep. 2022, ISSN: 1424-8220. DOI: 10.3390/S22197405. [Online]. Available: https://www.mdpi.com/1424-8220/22/19/7405/htm%20https://www.mdpi.com/1424-8220/22/19/7405.

[22] S. Dussy, D. Durrant, T. Moy, N. Perriault, and B. Célerier, "Mems gyro for space applications overview of european activities," vol. 8, 2005, pp. 6232–6243, ISBN: 1563477378. DOI: 10.2514/6.2005-6466.

[23] ESA, *Experimental mems sensor passes in-orbit test on cryosat-2*, 2010. [Online]. Available: https://www.esa.int/Enabling_Support/Space_Engineering_Technology/Experimental_MEMS_sensor_passes_in-orbit_test_on_CryoSat-2.

[24] D. Durrant, H. Crowle, J. Robertson, and S. Dussy, "Sireus - status of the european mems rate sensor," *AIAA Guidance, Navigation and Control Conference and Exhibit*, 2008. DOI: 10.2514/6.2008-6992.

[25] *Miniature inertial measurement unit | honeywell*. [Online]. Available: https://aerospace.honeywell.com/content/dam/aerobt/en/documents/learn/products/space/datasheet/N61-1613-000-000_MIMU-ds.pdf.

[26] "Astrix ® 1000 series," 2018.

[27] *Enpulsion - a global reference in electric propulsion*. [Online]. Available: https://www.enpulsion.com/.

[28] M. Villemant, P. Sarrailh, and S. Hess, "Droplets emission from feep and colloids thrusters: Modelling of droplets dynamics and interaction with spacecraft body,"

[29] *Enpulsion nano r³ - enpulsion*. [Online]. Available: https://www.enpulsion.com/order/nano-r3/.

[30] *Large-satellite quality at a small-satellite price is written in the stars | argo project | results in brief | h2020 | cordis | european commission*. [Online]. Available: https://cordis.europa.eu/article/id/413485-large-satellite-quality-at-a-small-satellite-price-is-written-in-the-stars.

[31] P. F. M.L. van den Berg A.E. Lyngvi, "Interstellar heliopause probe technology reference study communication at large distances," vol. SCI-A/2007/54/IHP, 1 2007.

[32] J. Saeedi, "Feasibility study and conceptual design of missile-borne synthetic aperture radar," *IEEE Transactions on Systems, Man, and Cybernetics: Systems*, vol. PP, pp. 1–12, Jul. 2017. DOI: 10.1109/TSMC.2017.2718114.

[33] ESA. "Cool tech to almost double deep space data." (2021), [Online]. Available: https://www.esa.int/Enabling_Support/Operations/ESA_Ground_Stations/Cool_tech_to_almost_double_deep_space_data.

[34] S. N. e. a. Tuhina Raj Usha Tiwari. "Improving reflector antenna parameters via mesh technique: Design analysis using cst studio." (2023), [Online]. Available: https://doi.org/10.1007/s41870-023-01618-8.

[35] J. L. Timothy Pham, "Performance analysis of operational ka-band link with kepler," 2016. [Online]. Available: https://www.thinkmind.org/articles/spacomm_2016_2_30_20032.pdf (visited on 01/09/2024).

[36] J. N. e. a. Michael Zemba. "Three years of atmospheric characterization at ka/q-band with the nasa/polimi alphasat receiver in milan, italy." (2021), [Online]. Available: https://ntrs.nasa.gov/api/citations/20180003217/downloads/20180003217.pdf.

[37] A. < I. Surname, I. Surname, and I. Surname. "Ariana 6." (2023), [Online]. Available: https://www.arianespace.com/vehicle/ariane-6/ (visited on 12/28/2023).

[38] E. Moeini, S. M. Karimian, H. R. Najaf, and A. G. Esfahani, “Thermal performance evaluation of a fabricated multilayer insulation blanket and validity of cunnington-tien correlation for this mli,” *Cryogenics Journal*, 2016. [Online]. Available: https://bpb-us-w2.wpmucdn.com/u.osu.edu/dist/4/26599/files/2016/08/Cryogenics-Journal-Paper-2455sba.pdf.

[39] R. M. Ambrosi, H. Williams, E. J. Watkinson, *et al.*, “European radioisotope thermoelectric generators (rtgs) and radioisotope heater units (rhus) for space science and exploration,” *Space Science Reviews*, vol. 215, 8 2019. DOI: 10.1007/s11214-019-0623-9.

[40] TU Delft, “Aerospace Design & Systems Engineering Elements (AE1222-II) slides.”

[41] S. Spaugh. “Beyond plutonium-238: Alternate fuel for radioisotope thermal generators.” (2022), [Online]. Available: http://large.stanford.edu/courses/2022/ph241/spaugh1/ (visited on 01/09/2024).

[42] A. Menicucci, “On-board command and data handling slides for ae3524,” 2023.

[43] Frontgrade Gaisler, *Gr718b*, Sep. 2021. [Online]. Available: https://www.gaisler.com/doc/gr718/gr718b-ds-um-3_8.pdf (visited on 01/09/2024).

[44] P. Armbruster, *Spacewire links routers and networks ecss-e50-12a*, n.d. [Online]. Available: https://sci.esa.int/documents/34795/36289/1567254473902-BC-JAXA-SpW-Meeting_1.pdf (visited on 01/09/2024).

[45] Frontgrade Gaisler, *Dual-core leon3-ft sparc v8 processor*, Nov. 2023. [Online]. Available: https://www.gaisler.com/doc/gr712rc-datasheet-2_5.pdf (visited on 01/09/2024).

[46] Micross, *Space-grade ceramic mram*, n.d. [Online]. Available: https://www.micross.com/uploads/33e6ec2e-7295-4573-a5f3-9de1c7a8f038/Ceramic-MRAM-Update-WEB.pdf (visited on 01/09/2024).

[47] J. Bouwmeester, *Lecture notes - spacecraft technology (ae3534) command & data handling*, n.d. [Online]. Available: https://ocw.tudelft.nl/wp-content/uploads/1.0-Command-and-Data-Handling-Lecture-Notes.pdf (visited on 01/09/2024).

[48] European Space Agency. “Spacewire.” (n.d.), [Online]. Available: https://www.esa.int/Enabling_Support/Space_Engineering_Technology/Onboard_Data_Processing/SpaceWire (visited on 01/09/2024).

[49] European Space Agency. “Spacewire.” (n.d.), [Online]. Available: https://www.esa.int/Enabling_Support/Space_Engineering_Technology/Onboard_Computers_and_Data_Handling/SpaceWire (visited on 01/09/2024).

[50] CAES, *Spacewire explained in six pages*, 2010. [Online]. Available: https://caes.com/sites/default/files/documents/App-Note-SpaceWire-Explained-In-Six-Pages.pdf (visited on 01/09/2024).

[51] European Space Agency, *Microprocessors*, n.d. [Online]. Available: https://www.esa.int/Enabling_Support/Space_Engineering_Technology/Onboard_Computers_and_Data_Handling/Microprocessors (visited on 01/09/2024).

[52] COBHAM, *Leon/grlib sparc processor cores*, n.d. [Online]. Available: https://www.xilinx.com/publications/product-briefs/partner/cobham-leon-product-brief.pdf (visited on 01/09/2024).

[53] J. Andersson, M. Hjorth, F. Johansson, and S. Habinc, “Leon processor devices for space missions: First 20 years of leon in space,” in *2017 6th International Conference on Space Mission Challenges for Information Technology (SMC-IT)*, IEEE, 2017, pp. 136–141.

[54] NASA, *State-of-the-Art Small Spacecraft Technology*. Pressbooks, Jan. 2023, ch. 8. [Online]. Available: https://www.nasa.gov/smallsat-institute/sst-soa/ (visited on 01/09/2024).

[55] Everspin Technologies, *Comparing technologies: Mram vs. fram*, 2020. [Online]. Available: https://www.everspin.com/file/157445/download (visited on 01/09/2024).

[56] S.-P.
bibinitperiod D.-T. staff, “Margin philosophy for science assessment studies,” Jun. 2012. [Online]. Available: https://sci.esa.int/documents/34375/36249/1567260131067-Margin_philosophy_for_science_assessment_studies_1.3.pdf (visited on 01/09/2024).

[57] R. Smith. “Europe complains: Spacex rocket prices are too cheap to beat.” (2018-06-2), [Online]. Available: https://www.esa.int/Enabling_Support/Space_Engineering_Technology/Onboard_Computers_and_Data_Handling/SpaceWire (visited on 01/09/2024).

[58] SmartAsset, *Inflation calculator*, n.d. [Online]. Available: https://smartasset.com/investing/inflation-calculator#CB1tc66v4k (visited on 01/09/2024).

[59] J. Likar, J. Porter, M. Donegan, *et al.*, “Space radiation environment considerations for the interstellar probe mission,” in *2022 IEEE Aerospace Conference (AERO)*, 2022, pp. 1–16. DOI: 10.1109/AERO53065.2022.9843306.

[60] I. Jun, H. B. Garrett, and R. W. Evans, “Trapped particle environments of the outer planets,” *IEEE Transactions on Plasma Science*, vol. 47, no. 8, pp. 3923–3930, 2019. DOI: 10.1109/TPS.2019.2907069.

[61] E. Ecale, F. Torelli, and I. Tanco, “Juice interplanetary operations design: Drivers and challenges,” in *2018 SpaceOps Conference*, 2018, p. 2493.

[62] Frontgrade Gaisler, *Gr740 quad-core leon4ft sparc v8 processor*, 2023. [Online]. Available: https://www.gaisler.com/index.php/products/components/gr740 (visited on 01/09/2024).

[63] European Space Agency, *Gr740: The esa next generation microprocessor (ngmp)*, 2022. [Online]. Available: http://microelectronics.esa.int/gr740/index.html (visited on 01/09/2024).

[64] Google, 2024. [Online]. Available: https://www.google.com/finance/quote/EUR-USD?sa=X&ved=2ahUKEwjuh6Se8s-DAxWy1gIHHcgbBJ4QmY0JegQIBxAv&window=1Y (visited on 01/09/2024).

[65] CoinNews, 2023. [Online]. Available: https://www.usinflationcalculator.com/inflation/current-inflation-rates/ (visited on 01/09/2024).

[66] Frakoterm. “Multi-layer insulation (mli).” (2023), [Online]. Available: https://frakoterm.com/cryogenics/multi-layer-insulation-mli/#:~:text=MLI%20consists%20of%20radiation%20shield,the%20heat%20transfer%20by%20conduction.

A

Large figures

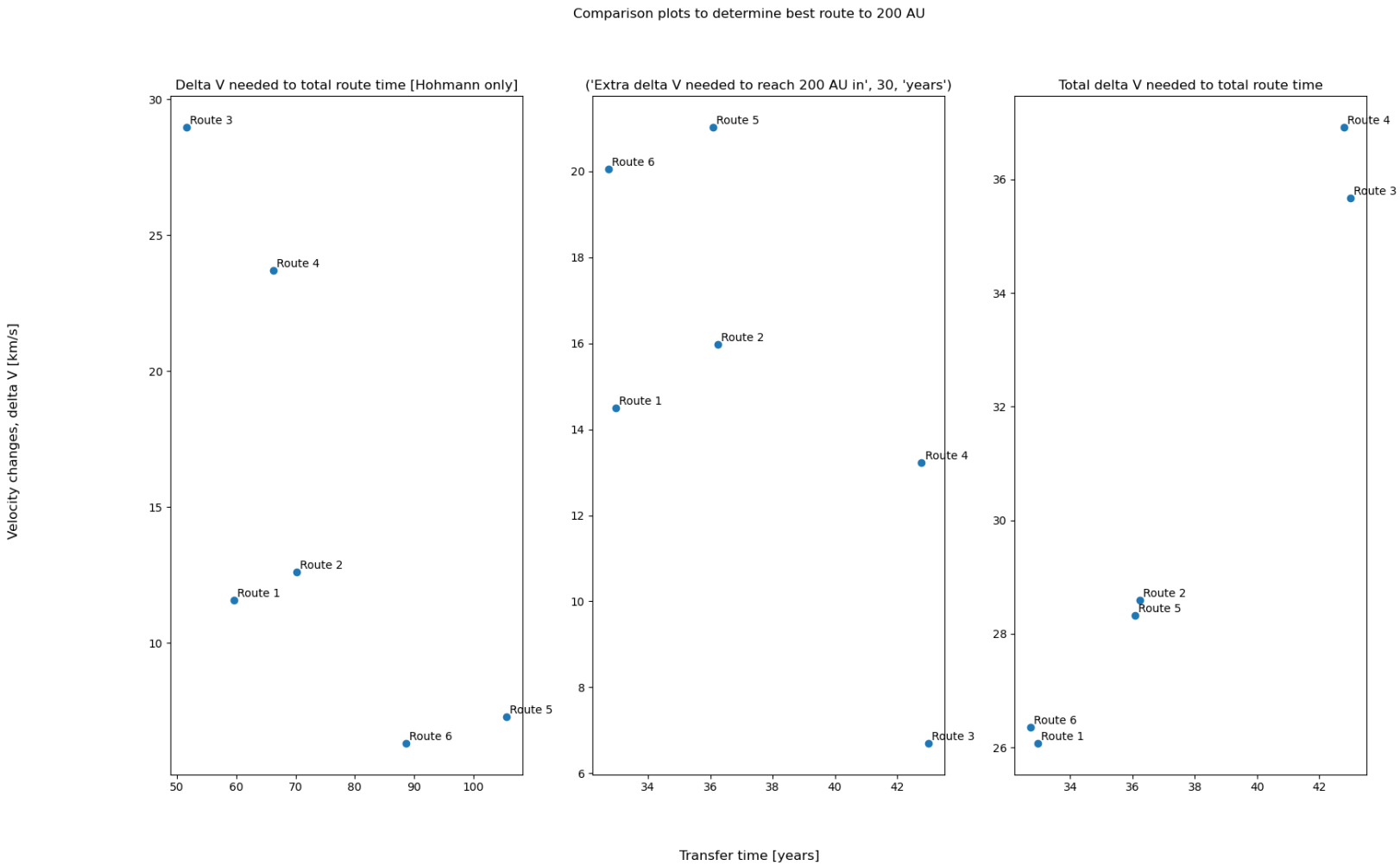

Figure A.1: Comparison of each route under the 30 year requirement

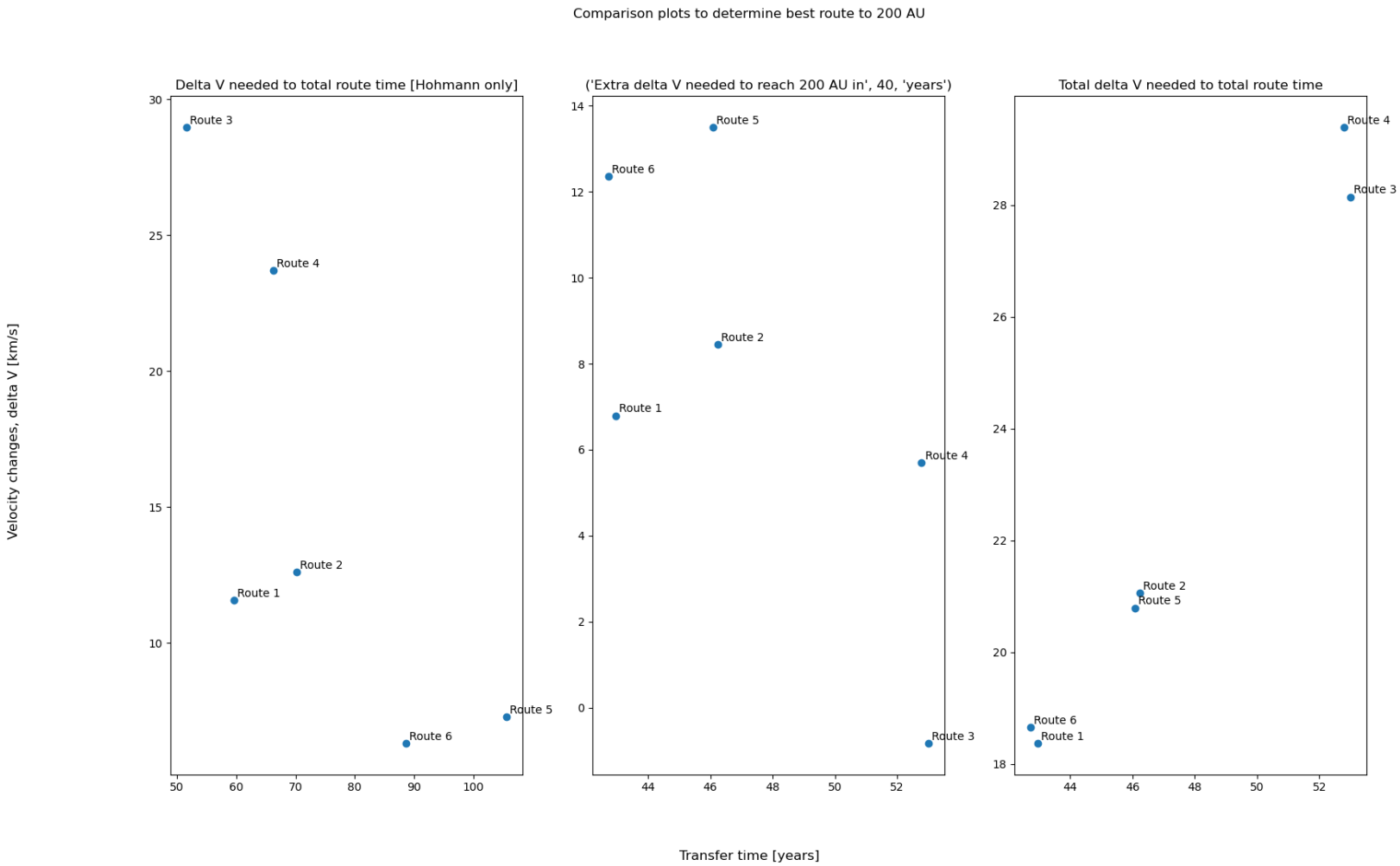

Figure A.2: Comparison of each route under a 40 year requirement

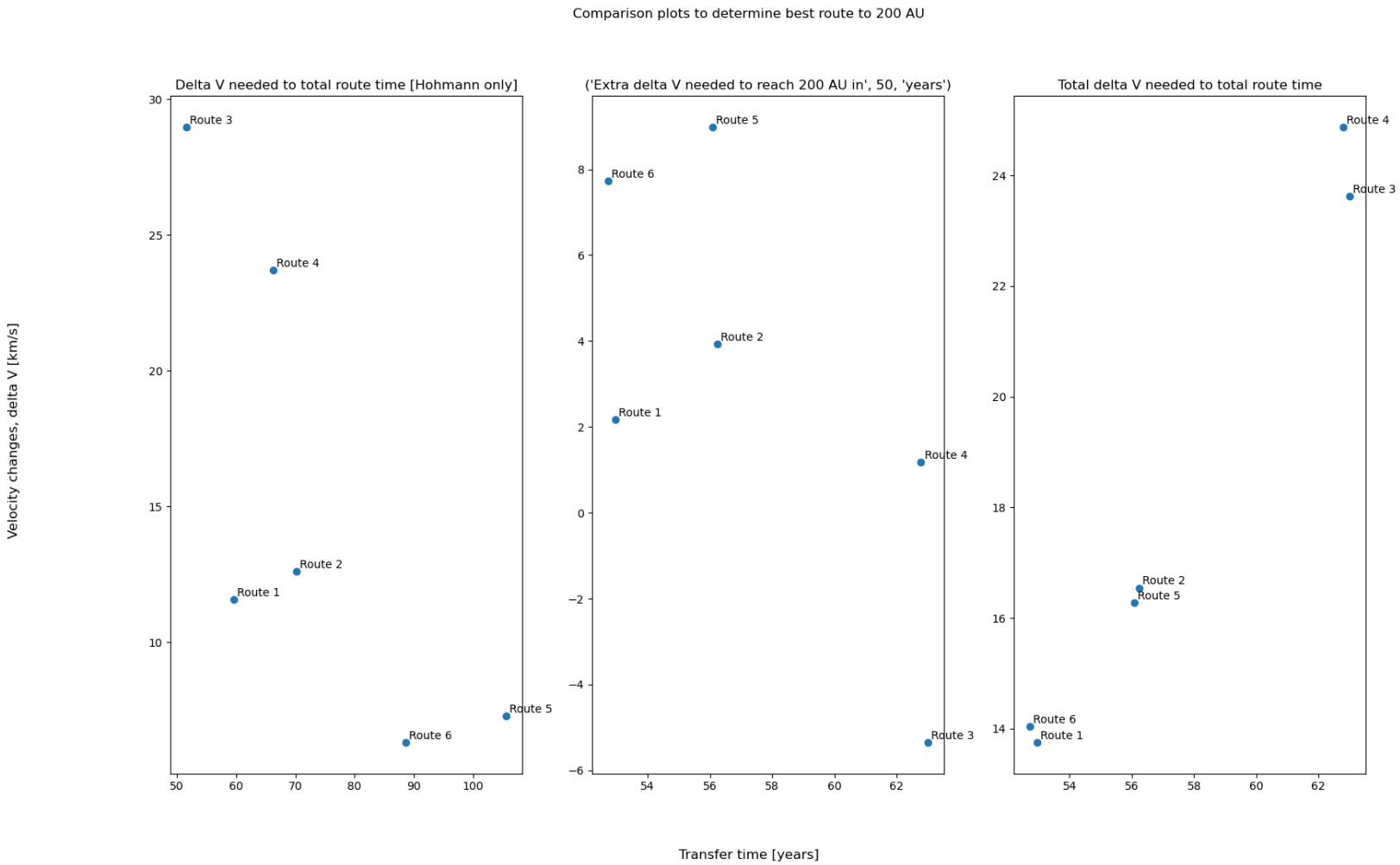

Figure A.3: Comparison of each route under a 50 year requirement

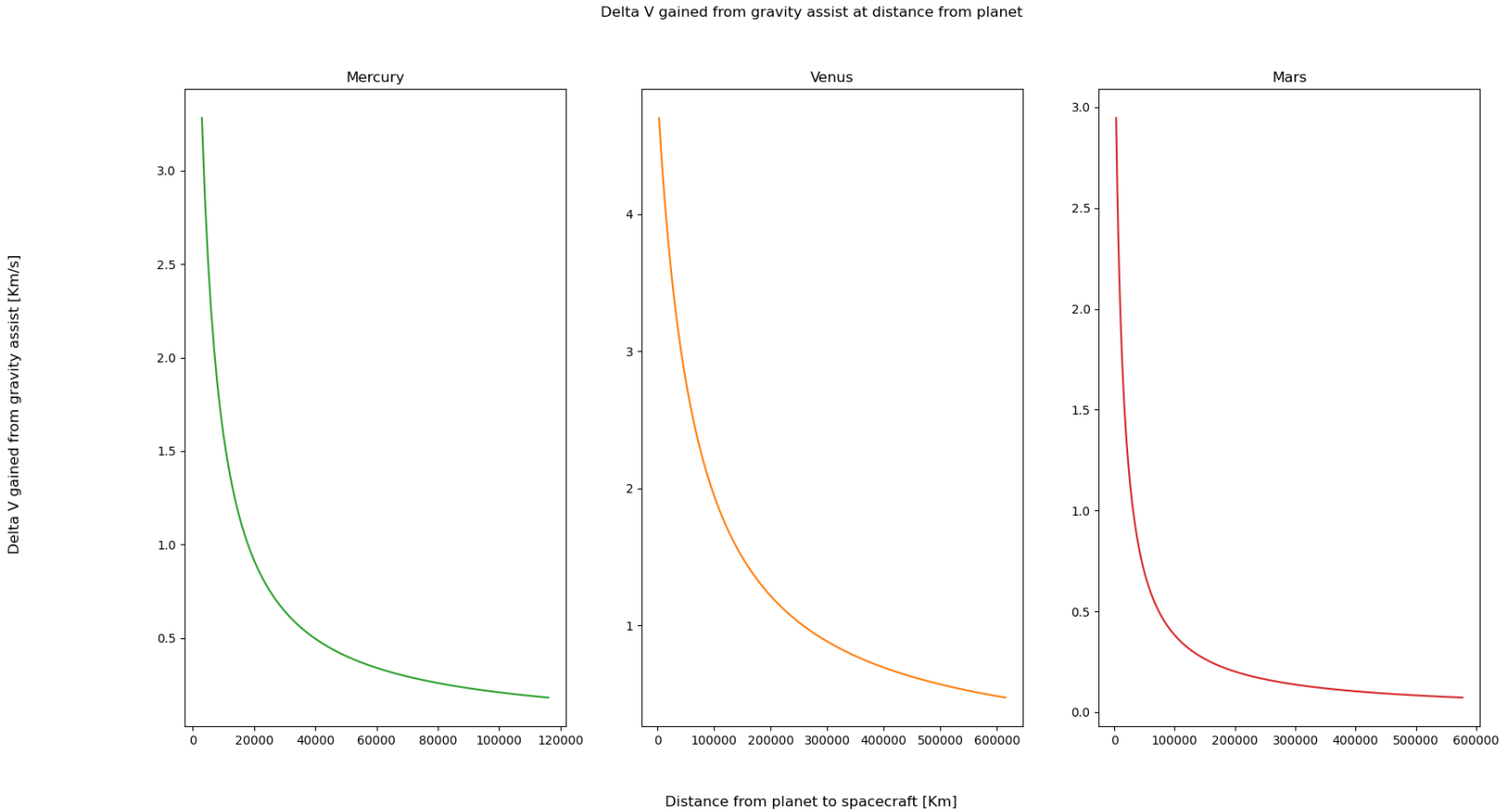

Figure A.4: Delta-V gained from gravity assist at distance from planet

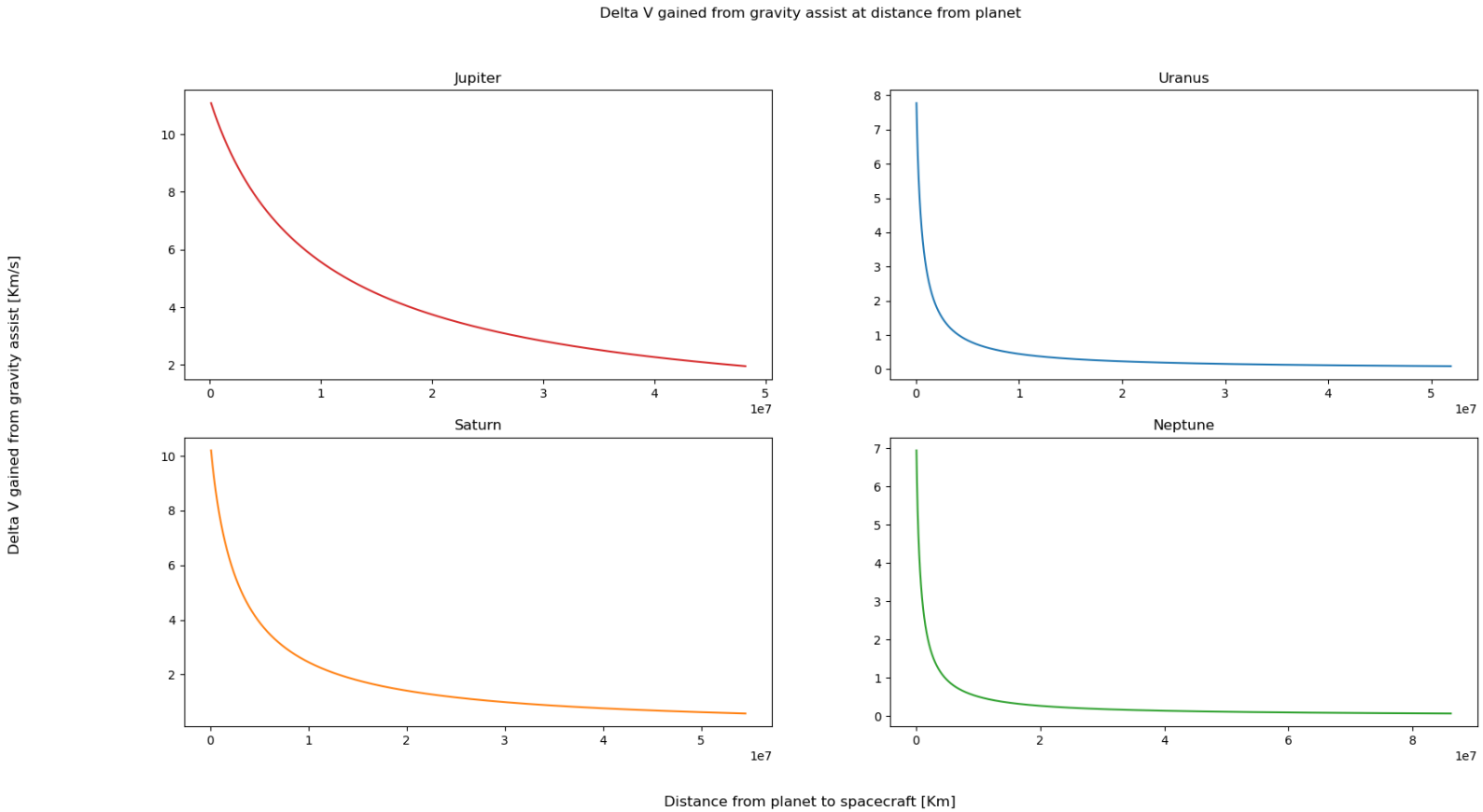

Figure A.5: Delta-V gained from gravity assist at distance from planet

derivation in reader

Sizing of RTG (radio-isotope thermal gen.)

- Characteristics
  - First US RTGs produced ~2.7W of electric power.
  - Recent RTG, generates ~290We @BOL and >200W @EOL
  - Thermal power is 4234 W, so efficiency 290/4234= 6.8%.
- For the power P at time t follows:

$$P \square P_0 \cdot e^{\left(\frac{-0.693}{\tau 1/2} \cdot t\right)}$$

$$M_{RTG} = \frac{P_o}{(P_{sp})_{RTG}}$$

Power Source	PBOL [We]	PEOL[We]	Mass [kg]	Dimensions [m]	Life[yrs]	Pu[kg]	Cost [M$]	TRL	Notes
Cassini RTG	285	210	55.5	D = 0.41,L=1.12	10.75	8	35.00	9	18 GPHS
New MMRTG	140	123	32	D = 0.41,L = 0.6	10	4	25.00	7	9 GPHS
SRG 1.0	114	94	27	D = 0.27,L = 0.89	3	0.9	20.00	4	2 GPHS

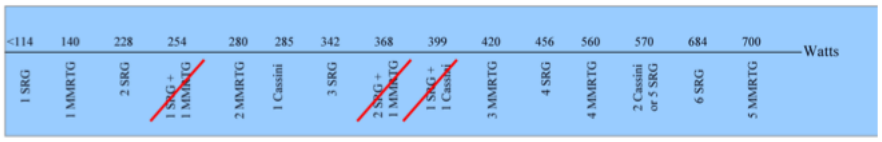

P_0 : initial power, P_{BOL}

$\tau_{1/2}$: half-life (the time it takes for P to be 1/2 of P_0)

$(P_{sp})_{RTG}$: RTG specific power [We/kg]

51
AE1222-II SC

Figure A.6: Slide from [40] on which the RTG sizing and design is based.

B

Python Code

The Python code for Orbit Determination is written by Jelle van der Meer: 4997476. Since the code file is around 600 Lines it is unnessecary to list every line therefore only the most important classes, functions and methods are given. Not all classes were used for the calculations, the ones used are the 'celestial dictionairy', 'hohmann transfer earth','hohmann transfer interplanetary' and 'maneuvers'.
For a full disclosure of the python code, contact Jelle van der Meer at J.H.C.vandermeer@student.tudelft.nl.
CODE:

```
    def circular_vel (gravitational_parameter, distance_r):
        circular_vel = math.sqrt(gravitational_parameter/distance_r)
        return circular_vel

    def escape_vel (gravitational_parameter, distance_r):
        escape_vel = math.sqrt((2*gravitational_parameter)/distance_r)
        return escape_vel

    def infinity_vel (gravitational_parameter, semi_major_axis):
        infinity_vel = math.sqrt(-gravitational_parameter/semi_major_axis)
        return infinity_vel

    def general_vel (gravitational_parameter, distance_r, semi_major_axis):
        general_vel = math.sqrt(gravitational_parameter*((2/distance_r)-(1/semi_major_axis)))
        return general_vel

    def hyperbolic_vel (escape_vel, infinity_vel):
        hyperbolic_vel = math.sqrt(escape_vel**2 + infinity_vel**2)
        return hyperbolic_vel

class orbital_parameters_elliptic:
    def distance_r (semi_major_axis, eccenctricity, true_anomaly):
        distance_r = (semi_major_axis*(1-eccenctricity**2))/(1+eccenctricity*math.cos(
            true_anomaly))
        return distance_r

    def periapsis_distance (semi_major_axis, eccenctricity):
        rp = semi_major_axis*(1-eccenctricity)
        return rp

    def apoapsis_distance (semi_major_axis, eccenctricity):
        ra = semi_major_axis*(1+eccenctricity)
        return ra

    def eccenctricity (periapsis_distance, apoapsis_distance):
        e = (apoapsis_distance-periapsis_distance)/(apoapsis_distance+periapsis_distance)
        if e < 0:
            print("The␣eccenctricty␣cannot␣be␣negative", ValueError)
        else:
            return e

    def orbital_period (semi_major_axis, gravitational_parameter):
```

```
42          orbital_period = math.pi * 2 * math.sqrt((semi_major_axis**3)/(
                gravitational_parameter))
43          return orbital_period
44
45  class orbital_parameters_parabolic:
46      def distance_r (gravitational_parameter, angular_momentum, true_anomaly):
47          distance_r = (angular_momentum ** 2 / gravitational_parameter) * (1/(1+ math.cos(
                true_anomaly)))
48          return distance_r
49      def periapsis_distance (angular_momentum, gravitational_parameter):
50          periapsis_distance = ((angular_momentum ** 2) / (2* gravitational_parameter))
51      def apoapsis_distance ():
52          value = "Infinity"
53          return value
54
55  class orbital_parameters_hyperbolic:
56      def elements (mu_body, v_sc_inf, rp, true_anomaly):
57          semi_major_axis = -(mu_body / (v_sc_inf * 2))
58          eccenctricity = 1 - (rp / semi_major_axis)
59          true_anomaly_limit = semi_major_axis*math.cos(-1/eccenctricity)
60          if eccenctricity > 1 and semi_major_axis < 0 and true_anomaly < true_anomaly_limit:
61              distance_r = (semi_major_axis*(1-eccenctricity**2))/(1+eccenctricity*math.cos(
                    true_anomaly))
62              return [semi_major_axis, eccenctricity, distance_r]
63          else:
64              #print("Initial parameters are not in accordance with a hyperbole")
65              return [semi_major_axis, eccenctricity, true_anomaly_limit]
66
67  class orbital_energy:
68      def energy (general_vel, gravitational_parameter, distance_r, semi_major_axis,
            eccenctricity):
69          kinetic_energy = 0.5 * general_vel ** 2
70          potential_energy = -gravitational_parameter / distance_r
71          total_energy = -gravitational_parameter / (2 * semi_major_axis)
72          characteristic_energy = gravitational_parameter/semi_major_axis
73          return [kinetic_energy, potential_energy, total_energy, characteristic_energy]
74
75  class celestial_dictionairy:
76      # Celestial data obtained from NASA's NSSDC fact sheets - date 9-12-2023
77      # Watchout for slight deviations from actual orbital parameters obtained from the
            poliastro module. Use the dictionairy for first-level approximations
78      sun_info = {"mass":1988500 * 10 ** 24, "diameter":696340, "radius":348170, "gravitational
            ␣parameter":132712 * 10 ** 6, "gravity":274.0, "escape␣velocity":617.6, "semi-major␣
            axis": "N.A", "orbital␣period":"N.A", "synodic␣period":"N.A", "orbital␣eccentricity":
            "N.A",}
79      mercury_info = {"mass":0.330 * 10 ** 24, "diameter":4879, "radius":2439.5, "gravitational
            ␣parameter":0.022032 * 10 ** 6, "gravity":3.70, "escape␣velocity":4.3, "semi-major␣
            axis":57.909 * 10 **6, "orbital␣period":88, "synodic␣period":115.88, "orbital␣
            eccentricity":0.206, "SOI": 0.117 * 10 ** 6}
80      venus_info = {"mass":4.87 * 10 ** 24, "diameter":12104, "radius":6052, "gravitational␣
            parameter":0.32486 * 10 ** 6, "gravity":8.9, "escape␣velocity":10.4, "semi-major␣axis
            ":108.210 * 10 ** 6, "orbital␣period":224.7, "synodic␣period":583.92, "orbital␣
            eccentricity":0.0068,"SOI":0.616 * 10 ** 6}
81      earth_info = {"mass":5.97 * 10 ** 24, "diameter":12756, "radius":6378, "gravitational␣
            parameter":0.39860 * 10 ** 6, "gravity":9.8, "escape␣velocity":11.2, "semi-major␣axis
            ":149.598 * 10 ** 6, "orbital␣period":365.2, "synodic␣period":"N.A", "orbital␣
            eccentricity":0.0167, "SOI":0.929 * 10 ** 6}
82      mars_info = {"mass":0.642 * 10 ** 24, "diameter": 6792, "radius":3396, "gravitational␣
            parameter":0.042828 * 10 ** 6, "gravity":3.7, "escape␣velocity":5.0, "semi-major␣axis
            ":227.956 * 10 ** 6, "orbital␣period":687, "synodic␣period":779.94, "orbital␣
            eccentricity":0.094, "SOI":0.578 * 10 ** 6}
83      jupiter_info = {"mass":1898 * 10 ** 24, "diameter":142984, "radius":71492, "gravitational
            ␣parameter":126.687 * 10 ** 6, "gravity":23.1, "escape␣velocity":59.5, "semi-major␣
            axis":778.479 * 10 ** 6, "orbital␣period":4331, "synodic␣period":398.88, "orbital␣
            eccentricity":0.049, "SOI": 48.2 * 10 ** 6}
84      saturn_info = {"mass":568 * 10 ** 24, "diameter":120536, "radius":60268, "gravitational␣
            parameter":37.931 * 10 ** 6, "gravity":9.0, "escape␣velocity":35.5, "semi-major␣axis"
            :1432.041 * 10 ** 6, "orbital␣period":10747, "synodic␣period":378.09, "orbital␣
            eccentricity":0.052, "SOI":54.5 * 10 ** 6}
85      uranus_info = {"mass":86.8 * 10 ** 24, "diameter":51118, "radius":25559, "gravitational␣
            parameter":5.7940 * 10 ** 6, "gravity":8.7, "escape␣velocity":21.3, "semi-major␣axis"
```

```
        :2867.043 * 10 ** 6, "orbital␣period":30589, "synodic␣period":369.66, "orbital␣
        eccentricity":0.047, "SOI":51.9* 10 ** 6}
86      neptune_info = {"mass":102 * 10 ** 24, "diameter":49528, "radius":24764, "gravitational␣
        parameter":6.8351 * 10 ** 6, "gravity":11.0, "escape␣velocity":23.5, "semi-major␣axis
        ":4514.953 * 10 ** 6, "orbital␣period":59800, "synodic␣period":367.49, "orbital␣
        eccentricity":0.010, "SOI":86.2 * 10 ** 6}
87
88  class hohmann_transfer_earth:
89      def delta_v (vel_circularD, vel_circularA, vel_transfer_per, vel_transfer_apo):
90          deltav_departure = vel_transfer_per - vel_circularD
91          deltav_arrival = vel_circularA - vel_transfer_apo
92          deltav_total = deltav_departure + deltav_arrival
93          return [deltav_departure, deltav_arrival, deltav_total]
94
95  class hohmann_transfer_interplanetary:
96      def delta_v (mu_sun, mu_body_dep, mu_body_tar, rdep, rtar, r_sc_0, r_sc_3):
97          vdep_planet_helio = math.sqrt(mu_sun/rdep) #vdep
98          vtar_planet_helio = math.sqrt(mu_sun/rtar) #vtar
99          vc0_sc = math.sqrt(mu_body_dep/r_sc_0) #vc0
100         vc3_sc = math.sqrt(mu_body_tar/r_sc_3)#vc3
101         atrans = (rdep + rtar) / 2
102         etrans = (abs(rtar - rdep))/(rtar + rdep)
103         vdep_sc_helio = math.sqrt(mu_sun * ((2/rdep) - (1/atrans))) #V1
104         vtar_sc_helio = math.sqrt(mu_sun * ((2/rtar) - (1/atrans))) #V2
105         vdep_sc_inf = abs(vdep_sc_helio - vdep_planet_helio) #vinf_1
106         vtar_sc_inf = abs (vtar_sc_helio - vtar_planet_helio) #vinf_2
107         vdep_sc_hyp = math.sqrt((2*mu_body_dep/r_sc_0) + (vdep_sc_inf ** 2)) #V0 hyperbolic
                vel
108         vtar_sc_hyp = math.sqrt((2*mu_body_tar/r_sc_3) + (vtar_sc_inf ** 2)) #V3 hyperbolic
                vel
109         deltav_sc_dep = abs(vdep_sc_hyp - vc0_sc) #delta 0 (V0 - Vc0)
110         deltav_sc_tar = abs(vtar_sc_hyp - vc3_sc) #delta 3(V3 - vc3)
111         deltav_total = deltav_sc_dep + deltav_sc_tar #delta3 + delta 0
112         time_trans = math.pi * math.sqrt((atrans ** 3)/ mu_sun)
113         #print(vdep_planet_helio, vtar_planet_helio, vc0_sc, vc3_sc, atrans, etrans,
                vdep_sc_helio, vtar_sc_helio, vdep_sc_inf, vtar_sc_inf, vdep_sc_hyp, vtar_sc_hyp)
114         #total deltav to go from local orbit to local orbit, deltav needed to get into
                hohmann transfer, excess entry velocity sc, heliocentric spacecraft velocity,TOF
115         return [deltav_total, deltav_sc_dep, vtar_sc_inf, vdep_sc_inf**2, vtar_sc_helio,
                time_trans/(3600 * 24), atrans, etrans]
116
117 class maneuvers:
118     def gravity_assist (mu_body, rp, v_planet_helio, v_sc_inf):
119         semi_major_axis = -(mu_body / (v_sc_inf * 2))
120         eccenctricity = 1 - (rp / semi_major_axis)
121         theta_inf = math.acos(-1/eccenctricity)
122         delta_phi = 2 * theta_inf -  math.pi
123         v1 = math.sqrt(v_planet_helio ** 2 + v_sc_inf ** 2 - 2 * v_planet_helio * v_sc_inf *
                math.cos((math.pi / 2)- (delta_phi / 2)))
124         v2 = math.sqrt(v_planet_helio ** 2 + v_sc_inf ** 2 -2 * v_planet_helio * v_sc_inf *
                math.cos((math.pi / 2) + (delta_phi / 2)))
125         delta_v = v2 - v1
126         energy1 = (((v2 ** 2)/2) - ((v1 ** 2)/2))
127         energy2 = 2 * v_planet_helio * v_sc_inf * math.sin(delta_phi/2)
128         return [delta_v, theta_inf]
```

C

Command and Data Handling

Prepared by Fanni Fiedrich) and proof-read by Huub Reitsma

The following appendix provides some additional insight into considerations concerning the Command and Data Handling (C&DH) subsystem. First, an outline of the design approach is given. The section includes the considered driving requirements and general constraints for the subsystem. Afterwards, the calculations for the different budgets are provided in more detail.

C.1. Design Approach

A driving factor is the long mission lifetime needed to be able to reach the heliopause. Since the C&DH is mission critical, this requires the overall architecture as well as individual components to be highly reliable. For this reason, harsh radiation environments have to be mitigated. In general, the components should be chosen with a focus on radiation hardening, providing protection against for example the effects of the Total Ionising Dose (TID), Single Event Latchups (SEL) and Single Event Upsets (SEU). Additionally, the operating temperature has to be taken into account for the components.

The trajectory goes through multiple different regions with varying space environments [59]. Solar particles, solar wind plasma and Galactic Cosmic Rays (GCRs) are the main sources of radiation, varying in intensity over the mission. The spacecraft encounters the strongest radiation environment during the Jupiter gravity assist, or at Saturn if no Jupiter gravity assist is used [59], [60]. The radiation during a gravity assist is dominated by electrons and protons trapped in the magnetosphere [60].

The data rates also put constraints on the C&DH subsystem. The memory storage and the processor choice depend on how much science data is produced and on how long it needs to be stored. The payload data rate, as well as the transmission windows and data bandwidth determine these factors. The payload is a highly integrated instrument suite developed by ESA. The instruments generate between 70 and 270 bits per second with one measurement cycle per hour [11]. More details on the up- and downlink data rates are provided in chapter 6.

Overall, the design process is approached by first gaining insight into mission concepts for interstellar probes. The main focus is laid on the ESA study, as it serves as a baseline for the project [11]. Since the description of the system is high-level in the study, more detailed research is needed. It is also important to keep technological advances in mind. To this end, the C&DH subsystems of the New Horizons and JUICE missions are taken as reference as well [15], [61]. These missions specifically are of interest since they visited outer solar system planets. The Voyager missions are not closely considered due to their age. The final design of the architecture is closely linked to the Interstellar Probe study design developed by researchers at the John Hopkins institute [16].

C.2. Processor Alternative GR740

The most up-to-date LEON-core technology on the market is a LEON4 quad-core LEON4 processor [62], [63]. It is referred to as the Next Generation Multipurpose Processor (NGMP) and the design is branded as GR740. As of 2022 it is QML-V qualified and certified by DLA [63]. The reason this

component is not chosen, is that a dual-core processor should be sufficient for the mission's processing needs. The LEON3-FT SoC is expected to be less expensive, and is therefore used in the system instead.

C.3. Detailed Calculations

The following sections give more detailed calculations for the mass, cost and power budgets.

C.3.1. Mass Memory Calculations

In order to calculate how much mass memory is required for the science data, a worst-case accumulation of data over six weeks is considered.

- **Instrument bps**: 70-270 bps with 1 measurement per hour
- **Data accumulated over 2 weeks**:
  - $1\ week = 60 \cdot 60 \cdot 24 \cdot 7\ s = 604800\ s$
  - Multiplying with data rate gives: $84,672,000$ to $326,592,000\ bit$
  - Assume: $8 \cdot 10^9\ bit = 1\ GB$
  - This gives: 0.010584 to $0.020412\ GB$
- **Worst-case scenario over 6 weeks**: 0.031752 to $0.122472\ GB$
- **With margin of 50%** [56]: 0.047628 to $0.183708\ GB$

C.3.2. Cost Budget Estimate

Cost estimates calculated for the year 2024 in € are given in Table C.1. To arrive at the cost in 2024, an inflation calculator is used [58]. The conversion rate from € to $ is estimated as 1.1 in 2024, though it is fluctuating over time [64].

The values for the New Horizons subsystem as well as the John Hopkins design are both taken from the John Hopkins study [16]. The initial values are in 2025 $. An inflation rate of 3.1% for 2024 to 2025 is assumed [65].

The SMAD high level Rough Order Magnitude (ROM) estimate is calculated as $883.7 \cdot 9^{0.491} \cdot 1000 + 26916 \cdot 1000 = 29,515,189.4$ for the year 2010. This is considering the full TTC subsystem, in which SMAD includes the CD&H subsystem [13]. Therefore, the result is higher than it would be only for the CD&H subsystem. The final value is a sum of a ROM estimate for the production and development costs. Additionally, it is important to note that the ROM estimate does not take costs of the software into account.

Source	Initial value	Calculation	Value [€ in 2024]
SMAD	$29,515,189.4$ $, 2010	$29,515,189.4 \cdot \frac{1.43857}{1.1}$	$38,599,696.38$€
New Horizons	$29,000,000$ $, 2025	$29,000,000 \cdot \frac{0.969932}{1.1}$	$25,570,934.55$€
John Hopkins	$57,000,000$ $, 2025	$57,000,000 \cdot \frac{0.969932}{1.1}$	$50,260,112.73$€

Table C.1: Calculations for a ROM cost estimate of the TTC subsystem (including C&DH) using SMAD, and calculating the costs estimated for New Horizons and in the John Hopkins study to € in 2024 [13], [16].

From the above, and the restrictions concerning the SMAD budget, the final cost is estimated to be around 40M € in 2024 economic conditions.

C.3.3. Power Budget Estimate

The power budget calculations for the C&DH subsystem use the datasheets for the SoC and router as reference [43], [45]. For the processor, a worst case-scenario is assumed in which both cores are fully powered at 100 MHz and two active SpaceWire links. The SpaceWire links are needed for the connection to the routers. Cold sparing is calculated with one element being fully powered, and the other being in standby mode. However, the specific router in the datasheet does not support cold

sparing. Therefore, the calculation is only to indicate what the approximate power consumption would be in a general case.

Processor Power Usage

Processor fully powered, both cores, 100 MHz, 2 SpaceWire links:
Typical: $1.5W + 2 \cdot 0.1W = 1.7W$
Maximal: $2.4W + 2 \cdot 0.15W = 2.7W$
Processor fully powered, one core, 100 MHz, 2 SpaceWire links:
Typical: $1W + 2 \cdot 0.1W = 1.2W$
Maximal: $1.5W + 2 \cdot 0.15W = 1.8W$
Processor on standby, 100 MHz:
Typical: $0.4W$
Maximal: $0.6W$
With hot standby (assume 2 cores) therefore:
Typical: $2.1W$
Maximal: $3.3W$
With cold standby (assume 2 cores) therefore:
Typical: $1.7W$
Maximal: $2.7W$

Router Power Usage

Full supply power ($V \cdot A = W$):
Typical: $0.75 \cdot 1.8 + 5/1000 \cdot 1.8 + 450/1000 \cdot 3.3W = 2.844W$
Maximal: $1 \cdot 1.8 + 15/1000 \cdot 1.8 + 600/1000 \cdot 3.3W = 3.807W$
Standby power ($V \cdot A = W$)[1]:
Typical: $2/1000 \cdot 1.8 + 350/1000 \cdot 3.3 + 1/1000 \cdot 3.3W = 1.1619W$
Maximal: $50/1000 \cdot 1.8 + 450/1000 \cdot 3.3 + 10/1000 \cdot 3.3W = 1.608W$
Hot standby:
Typical: $4.0059W$
Maximal: $5.415W$
Cold standby:
Typical: $2.844W$
Maximal: $3.807W$

Cold vs. Hot Sparing

Both router and processor in hot standby:
Typical: $4.0059 + 2.1W = 6.1059W$, with margin: $7.32708W$
Maximal: $5.415 + 3.3W = 8.715W$, with margin: $10.458W$
Only processor in hot standby:
Typical: $2.844 + 2.1W = 4.944W$, with margin: $5.9328W$
Maximal: $3.807 + 3.3W = 7.107W$, with margin: $8.5284W$
Both in cold standby:
Typical: $2.844 + 1.7W = 4.544W$, with margin: $5.4528W$
Maximal: $3.807 + 2.7W = 6.507W$, with margin: $7.8084W$

Memory Power Usage

The power usage of MRAM is assumed to be $900mW$ for writing one package of 1MB [54]. For most use-cases this amount of data should be sufficient for one writing operation. In the assumed worst case, it could span two packets simultaneously. Therefore, a maximum power usage of $1.8W$ is estimated. With a margin of 20% this gives $2.16W$.

Final Power Budget

The remainder of the $15W$ power budget can be used for SpaceWire components. After subtracting the necessary maximum power for hot sparing of both the router and the processor, this gives $15W - 10.458W – 2.16W = 2.382W$. Considering the margin of 20%, $1.985W$ remain. It is difficult to

[1] Due to uncertainties surrounding terminology, $I_{DDIOS\_LVDS\_E}$ and $I_{DDIOS\_LVDS\_D}$ are both included.

estimate the power needed for the SpaceWire components. Here, a maximum power budget of $15W$ is considered feasible for the C&DH subsystem, also since the ESA study considers it possible for a similar subsystem design [11]. Additionally, advances may be made concerning power usage of the used components until the integration of the subsystem.

D

Thermal control estimations

The following appendix gives an overview of the calculations that have been done for estimating the mass, power and cost of the thermal subsystem

D.1. mass, power and cost estimations

Firstly, the power estimation is quite simple as, as is said in chapter 8, the thermal control is fully passive and thus does not require any power.

For the mass estimation, the analysis was a bit different. The different components of the thermal subsystem were assessed individually and the total mass of the subsystem is the sum of these individual components. For the multi-layer insulation a density of $0.6kg/m^2$ was found by estimating the mass of a similar MLI product of a Polish company called Frakoterm [66]. With a necessary area of $12.4m^2$ this comes to a total mass of $7.44kg$ for the multi-layer insulation. For the total mass of the subsystem including loosely coupling the RTG and decoupling the antenna the mass comes to $15kg$. Adding a 20% margin to the total gives a final mass of $18kg$.
In terms of estimating the cost, formulas were used from the textbook: "Space mission engineering: the new SMAD" [13]. In this book the following formula was found:

$$Y = 646 * X^{0.684} \tag{D.1}$$

In this equation, Y is the non-recurring cost of the subsystem in 2010 thousand dollars, and X is the mass of the thermal control subsystem. In this cost estimation a conversion factor of 1/1.1 was used to convert the 2010 dollars to euros. This gave an estimated cost of 4.2 million euros for the thermal subsystem.

E

Structures estimations

The following appendix gives an overview of the calculations that have been done for estimating the mass, power and cost of the structures subsystem. Finally it also shows different views on a CAD model of the primary structure.

E.1. mass, power and cost estimations

For the mass estimation first the mass of the material used was calculated. The density of the chosen aluminum alloy 5052 is $2.67 * 10^3 \frac{kg}{m^3}$. The total volume of the materia can be calculated knowing the geometry.

$$V_{topplate} = V_{bottomplate} = length * width * thickness - 4 * corners$$
$$V_{sideplates} = 4 * heigth * radius * thickness + 4 * height * lengthcorner * thickness$$
$$V_{cylinder} = \pi * diameter * thickness * length$$
$$V_{deck} = \sum(V_{topplate}, V_{bottomplate}, V_{sideplates})$$
$$V_{tot} = V_{cylinder} + V_{deck}$$
$$M_{tot} = V_{tot} * \rho$$

Filing in the values gives the following answers.

$$V_{topplate} = 2m * 1m * 0.002m - 4 * 0.002m * 0.25 * 0.75/2$$
$$V_{topplate} = 0.004m - 0.00075 = 0.00325m^3$$
$$V_{sideplates} = 4 * 0.1m * 0.5 * 0.002m + 4 * 0.1m * 0.79m * 0.002m$$
$$V_{sideplates} = 0.0004m + 0.000632m = 0.001032m^3$$
$$V_{cylinder} = \pi * 1m * 0.002m * 1m = 0.00628m^3$$
$$V_{deck} = 2 * 0.00325m^3 + 0.001032m^3 = 0.007532m^3$$
$$V_{tot} = 0.007532m^3 + 0.00628m^3 = 0.0138m^3$$
$$M_{tot} = 0.0138m^3 * 2.67 * 10^3 \frac{kg}{m^3} \approx 37kg$$

The total mass of the shell will be around $37kg$. Since a frame will be inside the shell this mass will be doubled. Finally for the deployment mechanisms and the booms an mass of $15kg$ is taken. The booms

itself are light weight with a 100 grams per meter. With a margin of 20%, the total mass of the structure sub system is around $106.8kg$

Next the power estimation is estimated with previous missions in mind. 40 W as peak seems enough for the deployment.
In terms of estimating the cost, formulas were used from the textbook: ”Space mission engineering: the new SMAD” [13]. In this book the following formulas were found for non recurring costs:

$$Y = 646 * X^{0.684}$$

The formula gives the cost (Y) in 2010 thousand dollars with X being the mass of the structure. Converting 2010 dollars to modern euros is dividing the total cost by 1.1. Filling in gives the following:

$$Y = 646 * 106.8^{0.684} * \frac{1}{1.1} \approx 14.3 milioneuros$$

The total cost will be around 14.3 million euros.

E.2. CAD Model

In SolidWorks an 3d model was made for the satellite.

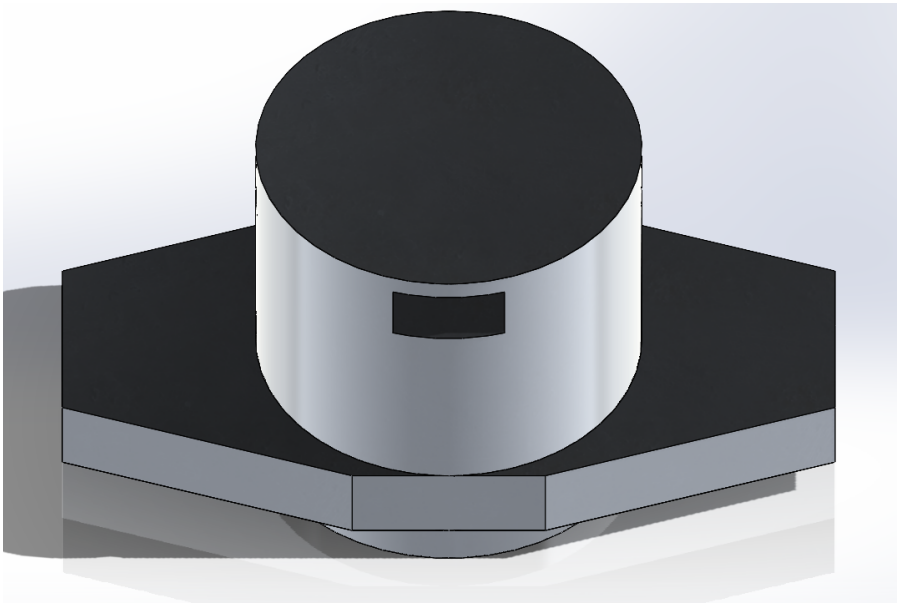

Figure E.1: A front top view of the CAD model

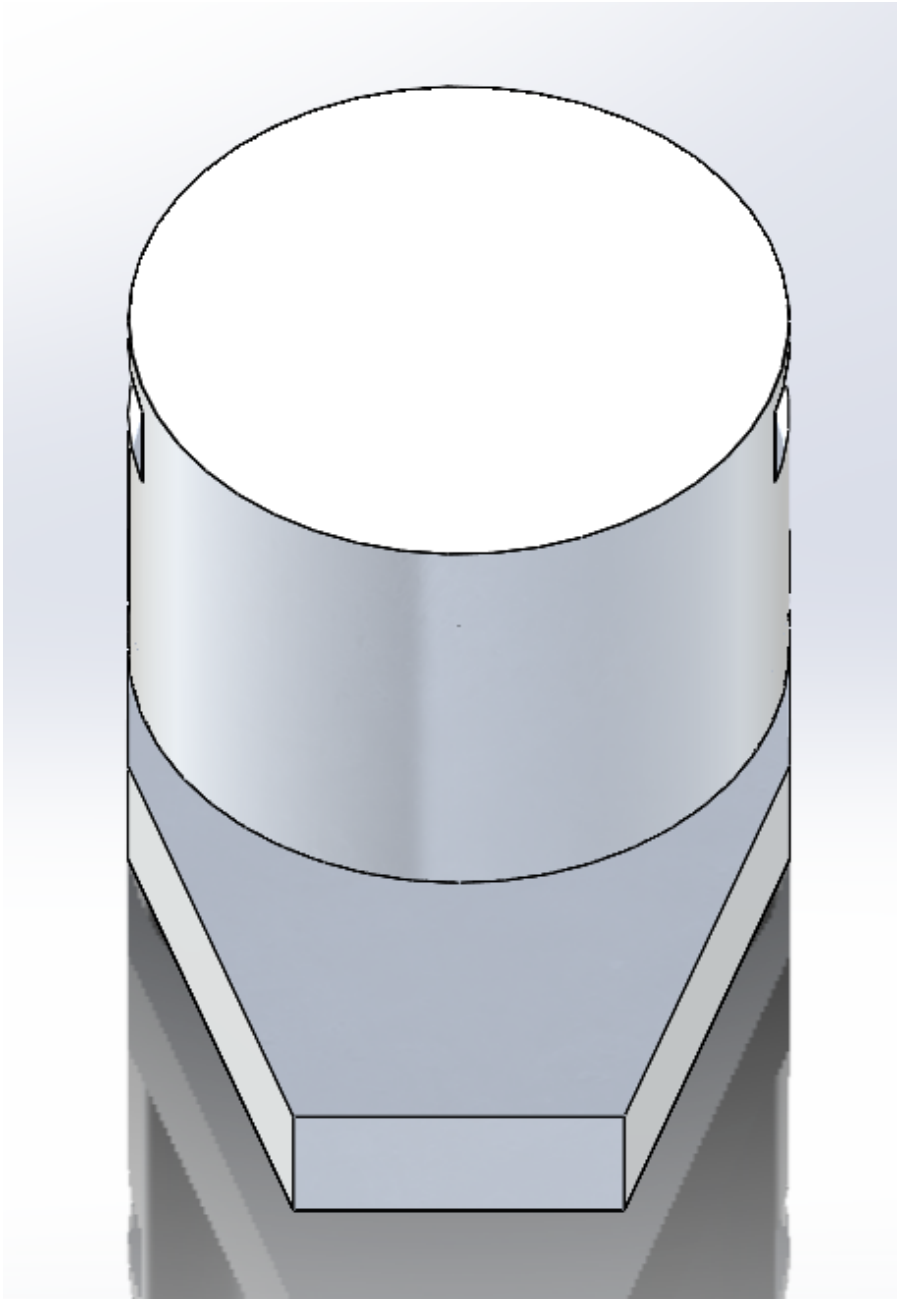

Figure E.2: A side top view of the CAD model

Figure E.3: A top view of the CAD model

F

Electrical Power estimations

The following appendix provides the calculations necessary for the design of the Electrical Power subsystem.

F.1. Mass and power estimations

We use the formula of radioactive decay to estimate the decrease in power over time as seen in [40] (or Figure A.6):

$$\mathrm{P(t)} = \mathrm{P}(0) \cdot e^{\frac{-\ln(2)\cdot t}{\tau_{0.5}}} \tag{F.1}$$

Where P(t) is the power at time t in years and $\tau_{0.5}$ is the half-life time of the system in years.

We found a half-life time of 53.54 years for the American design and a half-life time of 68.28 years for the European design when using Equation F.1 with the power decay per year. Combining this with a value of P(30) = 129 W (that is to say, the power after 30 years should be at least 129 W when looking at the power budget in Figure 9.1), we find using Equation F.1 and simple algebra that P(0) = 190.22 W for the American system and that P(0) = 174.9 W for the European system.

We then use that the specific power of the American system is 4.375 watts of electrical power per kilogram and that the specific power of the European system is 2 watts of electrical power per kilogram, resulting in a mass of 43.5 kg for the American system versus 87.45 kg for the European system. The result is that the European system is more than twice as heavy, which would heavily impact the mass of the total spacecraft and would cause a major increase of the solar sail. Since the solar sail is already a critical point of the spacecraft, it was decided that a European design is not feasible.

Since we continue with the design of the American RTG system, we check the requirements. After 5 years, the RTG power is around 178.3 W. This is still more than enough for the system to operate all of it functions (up to 151.2 W of usage), and since the solar sail will be deployed within this time the maximum power usage of the spacecraft becomes 129 W, which the RTG will be able to provide for the rest of the 30 year mission.

Since modern RTGs have an estimated thermal-to-electrical conversion efficiency of around 6.8% at the BOL [40] (see Figure A.6) and a maximum generated electrical power of 190.2 W at the BOL, we generate at most 3356.5 W of heat at the BOL. At the EOL (30 years after launch), we generate roughly 67.8% of the heat at BOL due to the decay of the nuclear fuel, which results in a BOL thermal power generated of around 2276.2 W.

We made some large but inevitable assumptions for the RTG system: we assume that we can model the decay of the system as a percentage per year, and we assume that the New MMRTG system will still function and be qualified after 30 years, even if the original lifetime lies around 10 years. We finally also assume that the New MMRTG can be dimensioned such that the power generated at BOL is equal to the necessary power. This will have to be researched further before committing to this design.